Delta and shelf clinoform development, the effect of sea level and sediment supply on geometry and time scales; an analogue flume model.

D.Wiersma

J.T. Eggenhuisen

Utrecht University

March 15, 2013

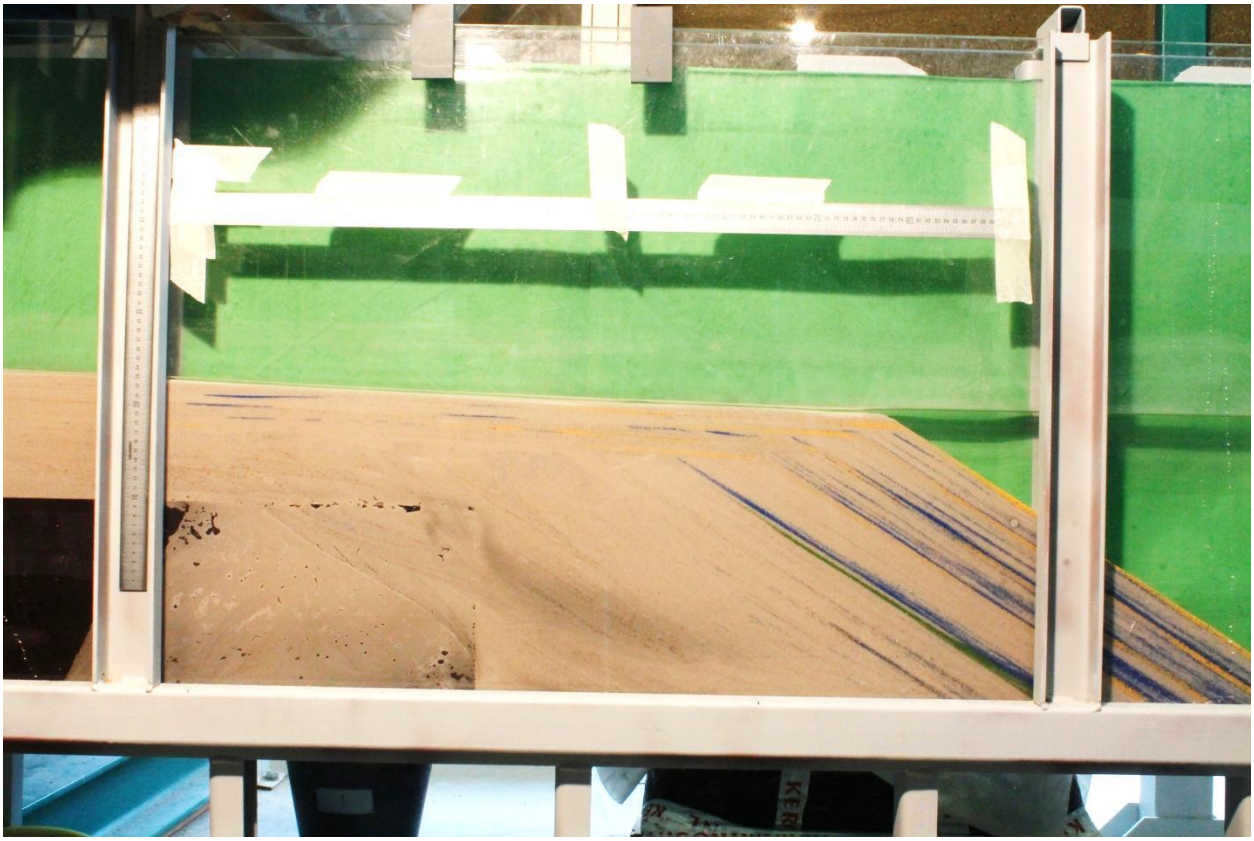

Abstract

Recent years have experienced a bloom in 2D analogue flume modeling, due to the clear and simplified representation it gives on sedimentary systems. The difference in spatial and temporal scales between delta and shelf clinoforms has often been disregarded in those experiments. Furtermore, both the shelf and the delta topsets have been approached as a static entity, rather than a dynamic transit system. Longitudinal profiles from both experimental and real world data sets show however, that characteristic slopes fluctuate with time. A set of simple experiments was conducted in a 2D flume, at the Eurotank Flume Laboratory, at Utrecht University. The experiments allow detailed observation of clinoform response to allogenic forcing, i.e. changes in sediment supply and base level. Changes applied with different frequencies indicate that the spatial scale of the system, dictates its sensitivity to changes applied at the time scales. Secondly, the system was able to change the gradient of the alluvial system with sea level change as sole driving mechanism. Changes observed in topset slope caused by sea level change are approximately 3 times larger than the changes produced by sediment supply. Comparison of the presented flume data, show that it is in agreement with data from large scale Quaternary alluvial systems.

Table of contents

1. Introduction

Basin infill may occur in the form of a continental shelf system that progrades. A continental shelf system can aggrade when a delta transits across its platform, and prograde when a delta is located at the shelf edge. In such periods transport of large quantities of sand towards the deeper parts of the basin is possible. Both deltas and shelf systems form clinoforms (Steel et al, 2008). The main difference between the two are the spatial and emporal scales at which they develop and all the processes that are involved on these time and spatial scales.

1.1 Shelf system.

Shelf margin clinoforms are considered the building blocks of continental shelves (Paola et al, 2009), they are several hundreds to a few thousand meters high, aggrade and prograde into bathyal water depths. Important segments of the shelf system are: shallow marine shelf platform, the shelf slope break (shelf edge), the bathyal slope and the transition from the slope to the basin floor (Steel et al, 2008).

Deltaic, estuarine and other shoreline settings commonly dominate the shallow marine platform, they transit across the platform at a rate that is dominated by sediment supply and formation of accommodation space. Shoreline morphology reflects the interaction between supply of sediment and basinal reworking processes. The principal processes that move sediment at shorelines are waves and tides. Where the shoreline is fed directly from a river that supplies sediment more rapidly than basinal energy can redistribute, a delta develops (Reading (1996)). Clinoform height of deltas is controlled by the drowning depth of the shallow marine platform, which in turn is related to platform slope and eustacy.

1.2 Sequence stratigraphy.

The processes that operate on both delta and shelf scale clinoforms can be described, explained and predicted using sequence stratigraphy. Sequence stratigraphy is uniquely focused on analyzing changes in facies and geometrical character of strata and identification of key surfaces to determine the chronological order of basin filling and erosional events (Catuneanu et al. (2009)). A sequence can be defined as product of sedimentation during a full stratigraphic cycle (of change in accommodation space or sediment supply), irrespective of whether all parts of the cycle are formed or preserved. In their attempt to standardize sequence stratigraphy, Catuneanu et al. (2009) recognize that a full stratigraphic cycle constitutes 2 sediment driven normal regressions during which the system progrades driven by sediment supply (high stand and low stand), a period of transgression during sea level rise and an episode of forced regression during sea level fall. These events result in the formation of a particular genetic type of deposits, known as system tracts (forced regressive, lowstand and highstand normal regressive and transgressive). This terminology suggests the preservation of a full sea level or sediment supply cycle. Furthermore, the direct identification of the system tracts skips the observational stage and jumps to immediate interpretation. Shoreline and shelf edge trajectory analysis provide an alternative method of analysis, to examine stratigraphic systems in a more descriptive way (Helland-Hansen et al. (2009) and Hendriksen (2009)). This methodology describes the formation of the different clinoforms, using accretionary and non-accretionary ascending and descending trajectories. The

superposition of sequences, system tracts or trajectories on one another, led to the development of a hierarchy in the analysis. This hierarchy is often placed in a framework of timescales that can be coupled to certain spatial scales and forcing mechanisms. First order cycles (10^9 -10^7 yr) are attributed to tectono-eustasy, e.g. formation and destruction of supercontinents. Second order cycles (10 – 80 Myr) and third order cycles (1 -10 Myr) are assumed to have typical sequence architecture with lowstand, transgressive and highstand system tracts and exposed surfaces as sequence boundaries. Fourth and fifth order sequences show simple sequences or parasequences (Schlager, 2010).

1.3 Transit time.

The most effective way to migrate a delta towards the shelf edge is during sea level low stand. Infill of the basin occurs as this system migrates basin ward (Steel (2008)). A delta located at the shelf edge is also considered one of the most favorable scenarios to pass large quantities of sand from the shelf to the deep water slope and basin floor. The mechanisms that drive the delta toward the shelf edge have received a lot attention in the past years. Recent work has shown that Pleistocene systems are often capable of migrating towards the shelf edge, during sea level highstand (Burgess and Hovius (1998)). The transit time describes the time needed for a specific fluvial system to drive the delta completely across a shelf, with a set gradient and width. Conventional models rely on base level fall to drive the delta to the shelf edge. However, modern delta systems can reach the shelf edge during sea level rise (Steel et al, 2008, Muto and Steel, 2002). Provided that the sediment supply is high enough to fill the created accommodation space, the delta will prograde over the shelf topset even during sea level rise. Delta transit time is dependent on delta and shelf topset and foreset slopes, rate of sea level rise and the width of the shelf. The dominant factor in determining whether the delta can reach the shelf edge is considered to be the non-erodable shelf slope (Muto and Steel (2002)).

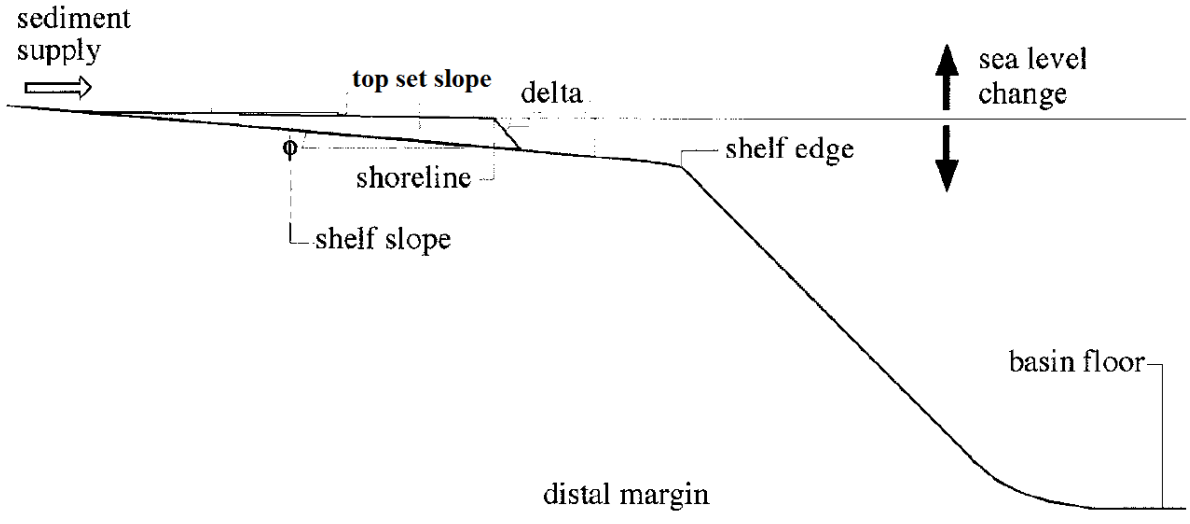

Figure 1.1, Schematic representation of a shelf system. The small clinofrom represents a delta that transits on the shallow marine platform (topset) of the larger shelf clinoform. Aggradation of the shelf occurs when the delta transits the platform and progradation of the shelf system occurs when the delta is located at the shelf edge. (modified after Muto and Steel (2002)).

1.4 Equilibrium time.

Every system can be described using its equilibrium time. This is the time a system needs to return to equilibrium after the boundary conditions have been modified. A system is in equilibrium when its shape remains constant over time. The equilibrium time can be approached with $T = L^2 / v$, where T is the equilibrium time (sec), L is the length of the system and v is the diffusivity (Paola et al, 1992 and Postma et al, 2008). When the boundary conditions change slowly compared to the equilibrium time, the system will react in a quasi-equilibrium manner. On the other hand, when the boundary conditions evolve rapid relative to the equilibrium time, the systems response will not be in equilibrium with the forcing. In such cases, a system might not respond in a straight forward manner to allogenic forcing.

1.5 Aims and objectives.

Understanding and proper characterization before mentioned processes, provide the foundation to evaluate the role of allogenic processes and their role on shelf margin growth (Carvaljal and steel, 2008). Recent years have seen a bloom of experiments in 2D experimental setup to develop a better understanding on the different forcing mechanisms working on delta and shelf systems (Paola et al, 2009). In these experiments the differences between delta and shelf systems have either been disregarded (Lai and Carpart 2007) or the shelf system has been approached as a static bounding entity, rather than a dynamic part of the sedimentary system (Muto, 2001, Muto and Steel, 2002 and Lorenzo-Trueba et al, 2009). Furthermore, these models often regard the alluvial system as a transit system that doesn't constitutes a large role. Thereby overlooking the buffering capacity of the subaerial slope (Holbrook et al, 2006).

Alternations in the gradient of the alluvial system over time are recognized for large river systems during the Cenozoic (Blum and Aslan, 2006 and Berendsen and Stouthamer, 2001) and are often attributed to changes in climate and sediment supply. However, this oversimplification doesn't regard the role of headward erosion and the autogenic tendency of the system to aggrade or degrade to its characteristic equilibrium slope. The dynamic reaction to applied changes of the sedimentary system, remain a topic of discussion. Can a dominant forcing mechanisms controlling the geometry of the clinoform, be recognized and what are the applications for preservation potential and delta transit times of delta systems towards the shelf?

Secondly, although the concept of equilibrium time is well established in the literature (Paola et al, 1992 and Postma et al, 2008), the application on a system operating on different spatial scales (shelf and delta system) is less understood. Questions remain about whether a time threshold can be defined at which a system is still sensitive to the applied forcing and what is the link between the spatial and temporal time scales that control allogenic forcing. Furthermore, can these time scales be coupled to any ordered hierarchy and known geological time scales.

In this report an attempt is made to address the posed questions. First, an analysis of new flume data is presented, to demonstrate the role of base level and sediment supply on the development delta and shelf clinoform. Special emphasis will lie on the geometry of the delta and shelf topset, the delta break and shelf edge trajectories and the response of the system to changes applied on different time scales. Secondly, to test the applicability in the field, the results will be compared to real world data.

2. Methods

2.1 Set-up

The research was conducted in the Eurotank Flume Laboratory, at Utrecht University. The experiments were conducted in an acrylic glass walled flume, 0.05m wide, 0.75 m high and 2 m long (fig. 2.1). The small width of the flume suppresses autogenic variability. Autogenic refers to the systems internal dynamics, such as meander formation or local incision. By decreasing the width of the flume the system will behave uniform over the its entire width, thus making it possible to study larger scale processes in a 2D model. This approach provides a clear view of the ways in which a simple shelf system responds to allogenic forcing. In this flume the water discharge, sediment input volume and water level (sea level) can be regulated, thereby simulating natural variations in relative sea level and climate in the hinterland. On the left side of the flume sediment and water were fed into a gravel basket, which ensures a calm and uniform entry of the sediment mixture to the tank. The discharge of water and sand could be adjusted through a tap with a flow meter and a screw feeder, respectively. The same sediment was used in all experiments, the sand has an average grainsize of 263.45 µm and consists of 99.7% of quartz. The water flows out of the flume via an outlet that is adjustable in height (fig 2.1), with an accuracy of 1mm, allowing application of a predetermined water level curve. A clinoform was allowed to develop and reach equilibrium, for approximately one hour with constant sediment supply of 2 l/hr, constant water discharge 200 l/hr and a constant sea level before the start of every experiment. Thereby creating stable equilibrium conditions and ensuring the same start conditions for all experiments.

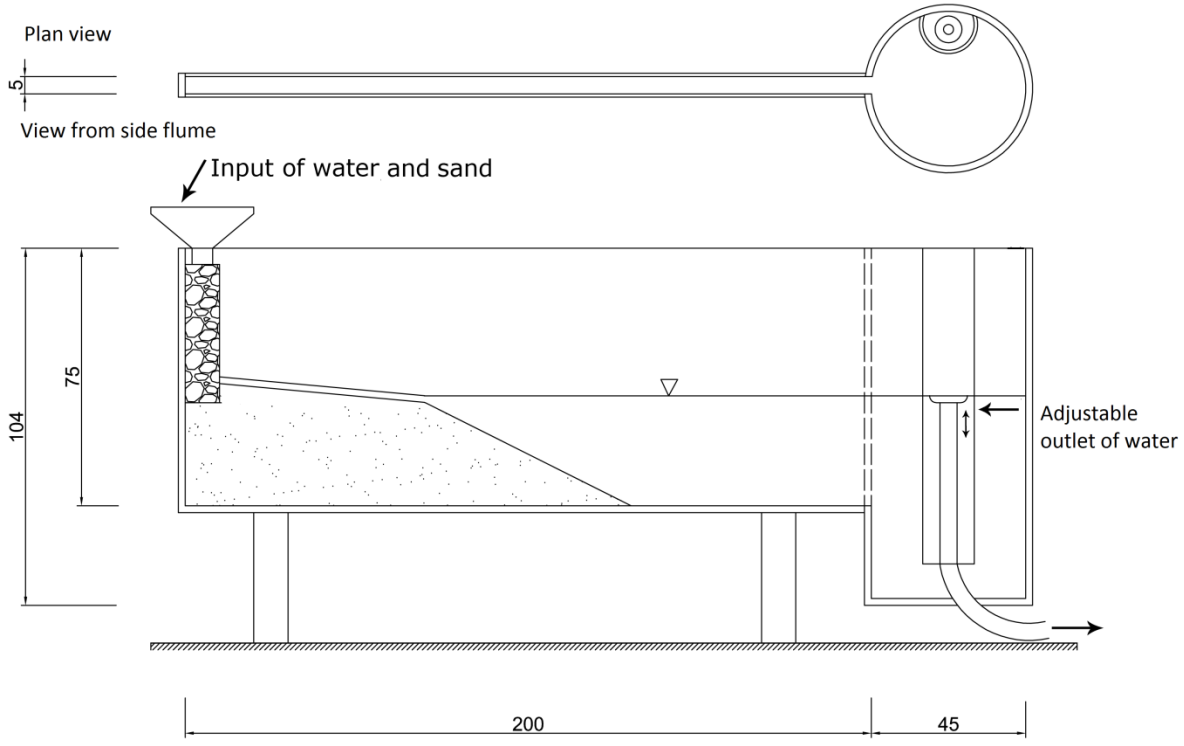

Figure 2. 1, Schematic drawing of the experimental flume. The sand body drawn in this figure resembles the clinoform at the start of every experiment (Modified after v. Noorden 2012). The view on the experiment was blocked in two locations along the wall of the flume, by beams set in place to support the acrylic glass window.

2.2 Boundary conditions.

2.2.1 Equilibrium runs.

To determine the boundary conditions of the flume a set of equilibrium runs were conducted, in the same flume, preceding the experiments. The aim of these experiments was to determine the time scales that are to be considered in these experiments (Appendix A).

The main finding of these equilibrium runs is that for a system of 1.16 m in length, the equilibrium time is approximately one hour. The equilibrium time of a system is the characteristic time scale at which the system responds to changes. To ensure that the applied changes will have an effect on the system, the high frequenty that was used has a period of one hour, the equilibrium time. To test the systems response to low frequency changes, a period of 4 hours, 4 times the equilibrium time, was used.

Furthermore, it was determined that a water discharge of 200 dm^3/hr provides the best equally distributed flow over the sediment surface for the entire range of sediment volumes used. The equilibrium slope that develops with a sediment supply of 2 dm^3/hr is 0.0414.

2.2.2 Experiments.

The experiments can be divided into 3 categories. First the three input variables sediment discharge and sea level, were varied separately, to gain understanding on their role in the formation of the shelf clinoform system. The third category combines a fluctuation in sediment supply with sea level change, to determine how the two interact. The special focus lies on the geometry of the system, the timing of sediment delivery to the shelf edge and the preservation of the top set.

Sea level experiments

First 5 experiments were conducted, where only the sea level was changed and the sediment supply and water discharge were held constant at 2 dm^3/hr and 200 dm^3/hr respectively. These experiments are referred to as the sea level experiments (SL).

Three high frequency experiments were conducted. The high frequency describes a sea level curve with a period of one hour, equal to the equilibrium time, and an amplitude of 1.25 cm (fig 2.2). The changes in sea level during the experiment are applied every 5 minutes. Especially during the rapid sea level rise this can result in extreme and instantaneous changes, rather than a smooth and continuous change. To test the impact of these changes, two identical experiments have been conducted. In experiment SL_HF_A1 the sea level changes are applied every 5 minutes and in experiment TR the changes are applied every minute. To investigate the effect of this difference on the system while the delta is located at the shelf edge as well as when the system is experiencing transgression, this test run conducted for an experiment with a sea level change with a high frequency. The TR run was performed for 100 min, which includes one entire transgression cycle. The term transgression cycle describes a period during which the delta has left the shelf edge, including transgression and regression. For the third high frequency experiment, SL_HF_A3, a linear sea level rise of 4 cm over 4 hours was superimposed on the earlier

described high frequency sea level curve (fig 2.2). Hereby, simulating subsidence and consequently increasing preservation potential.

During the sea level experiments, 2 different low frequency sea level curves, with a period of 4 hours and an amplitude of 1.25 cm, were applied; a simple curve with no subsidence component (SL_LF_A1), the same curve with the same subsidence component as used for the high frequency experiments (SL_LF_A3) (fig 2.2).

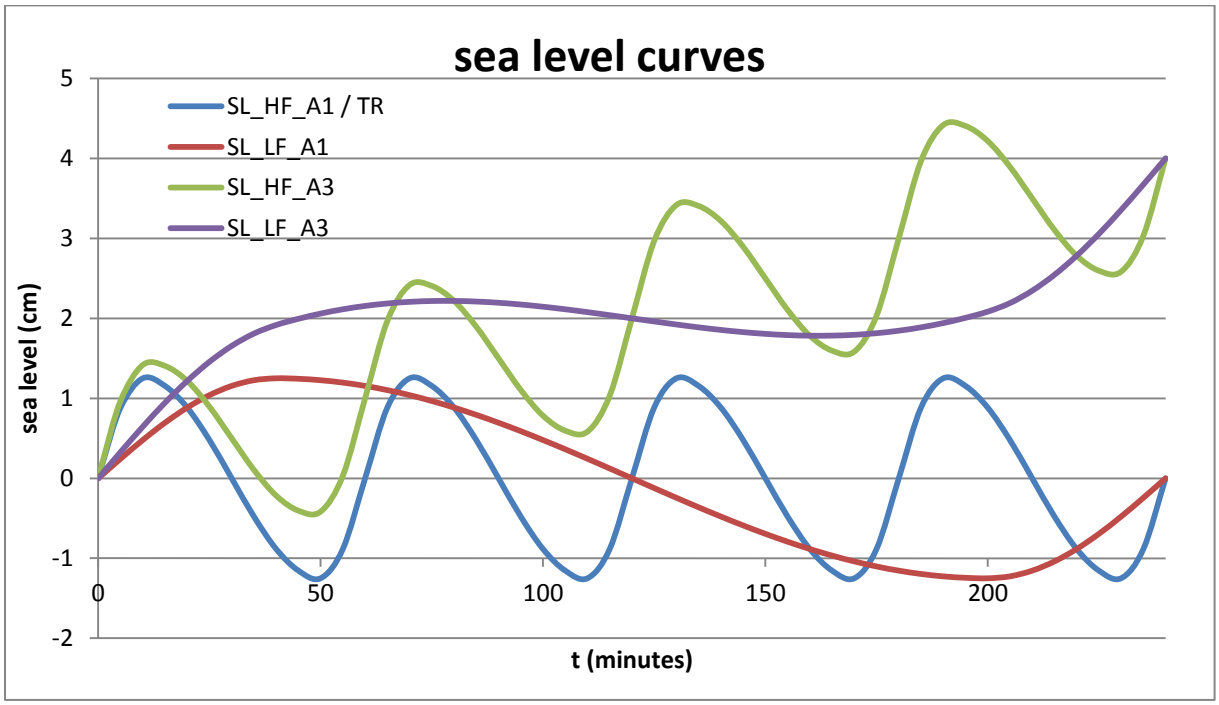

Figure 2. 2, Sea level curves used for the sea level (SL) experiments. Please note, that during the TR run and SL_HF_A1 run the same sea level curve was applied and only the interval of the applied changes was different. The TR run lasted 100 min, enough time to include exactly one transgression cycle.

The sea level curves used in the experiments are asymmetrical. This is an analogue to the growth and melting of ice sheets during the Cenozoic (Imbrie and Imbrie (1980) and Imbrie (1985)). According to Milankovich theory a rapid melting of the ice caused by summer insolation in the northern hemisphere led to fast sea level rise. The slow growing of the ice sheets would represent a much longer time period leading to a slow sea level fall.

Colored sand was added to the experiments at distinct times in the sea level curve. The green sand was added before the start of the experiment, the yellow sand during sea level low stand and the blue sand during sea level high. This enables the identification of which parts of the system are deposited and preserved during different stages of the experiment.

Sediment supply experiments.

In a second series of 3 experiments both the sea level and the water discharge (200 dm^3/hr) were constant, and the volume of sediment supplied to the system was changed. These experiments are

referred to as the sediment supply experiments (QS). Two high frequency curves were applied that are exactly out of phase with each other (QS_HF_A1 and QS_HF_A7) (fig 2.3). The period of these curves is one hour and the amplitude is 1 dm^3/hr, thus fluctuating between 1 and 3 liter sand added per hour. The curves used are asymmetrical, thus one experiment with fast increase and slow decrease in sediment supply and one in exact antiphase. Additionally, one low frequency curve was utilized (QS_LF_A1), the period of this curve is 4 hours and the maximum and minimum sediment discharge is equal to that of the high frequency sediment supply variations. The low frequency change in sediment supply is applied according to a symmetrical curve (fig 2.3).

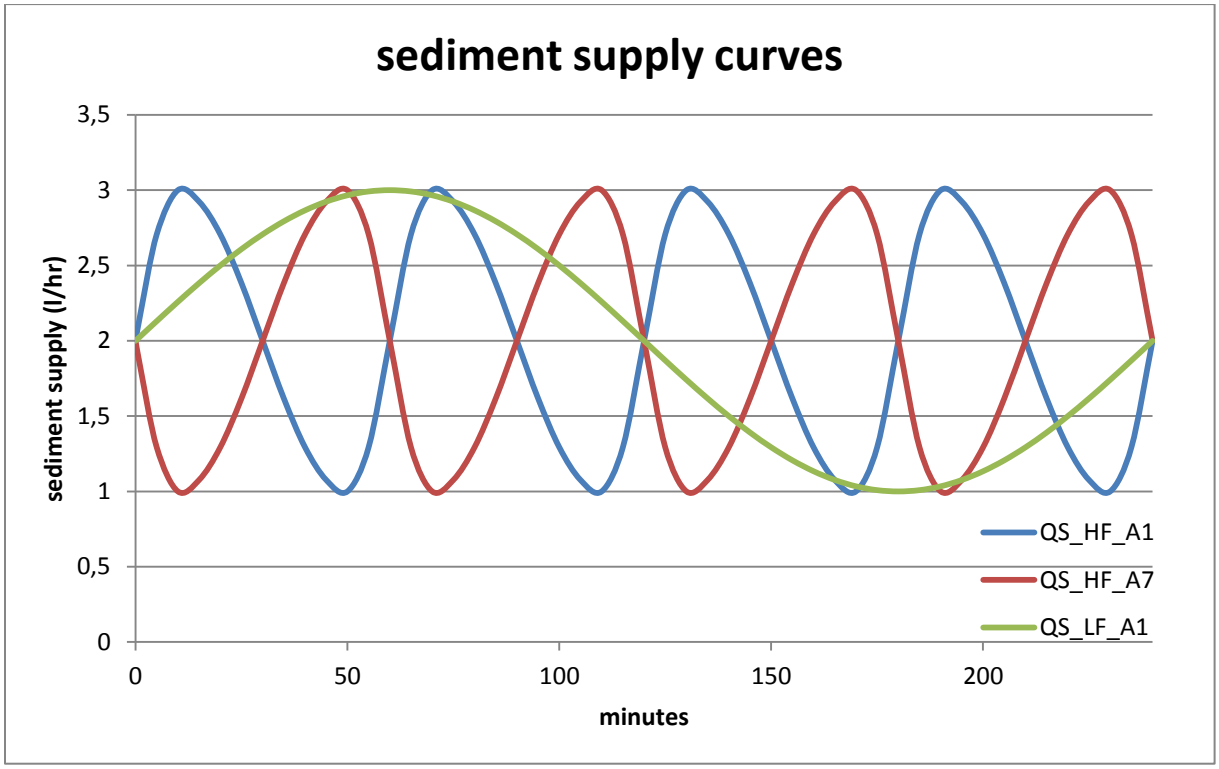

Figure 2. 3, sediment supply curves used in the sediments supply experiments.

Combined experiments.

To test how the input variables would interact a third set of experiments was conducted, in which both the sediment input and the sea level was changed. These experiments are known as the combined experiments (CO). To ensure transgression, the high frequency sea level curves are used in the combined experiments. To enhance preservation potential in these experiments, in all three of them a subsidence component, linear sea level rise of 1 cm/hr, was added to the sea level curve (fig 2.4). The difference between the three experiments is the sediment supply curve. The sediment supply curves used in the combined experiments are the same curves used in the QS experiments. The first curve is in phase with the sea level fluctuations (CO1_HF_A3), the second is in exact antiphase with the sea level curve (CO2_HF_A3) and the final sediment supply curve is a low frequency, symmetrical curve (CO3_HF_A3) (fig 2.4).

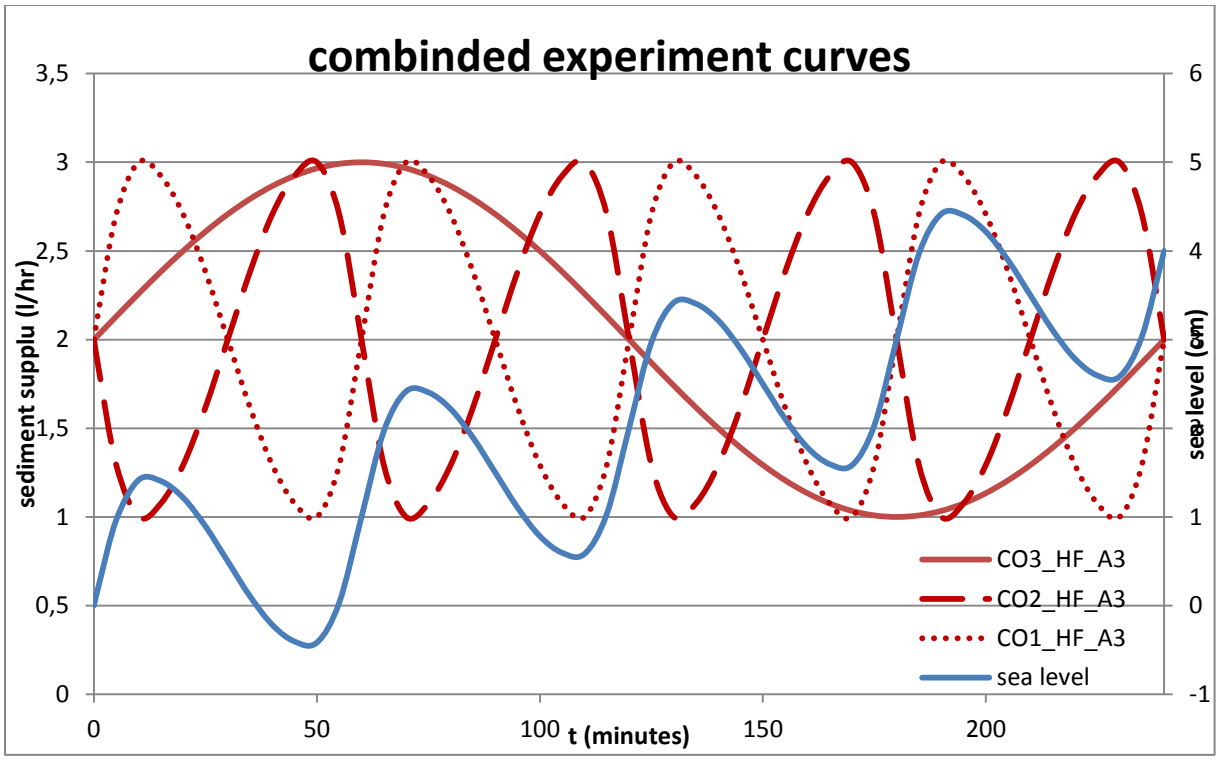

Figure 2. 4, The sediment supply curves that are used in the combined experiments are projected here in red. Please note the clear difference in symmetry between the high and low frequency curves. The blue line represents the sea level curve that was used in the combined experiments.

In the combined experiments also colored sand was added, at the same moments during the sea level curve as during the earlier experiments. A summary of all experiments conducted is given in appendix 2.

2.3 Analysis of the data.

To document the experiments, photos of the experiment were taken every 30 second. The photos were analyzed using MATLAB (fig. 2.5a). On every photo a series of operations were executed. First every pixel was assigned a value in correspondence with its color, thereby converting the photo into a matrix. The average value in horizontal direction, for columns of 10 pixels wide was calculated. After which the largest change in value between the averaged column width in the vertical direction was measured, i.e. the largest color shift and documented as the sediment surface. This was repeated over the entire width of the photo, thereby documenting the complete sediment surface for that moment in time. The location of the shelf break was determined by fitting two straight lines through the determined sediment surface using MATLAB (one through the topset and one through the foreset) and determining the intersection of these lines (fig. 2.5a). When the delta was located at the shelf edge, its position was documented in the same way. For the periods when the delta was not located at the shelf edge, the location of the delta was determined by the first location, left to right along the topset, where the slope between 2 points was larger than 0.06 (fig 2.5b). After determining the location of the delta, the average slope of the delta topset was calculated (fig 2.5c). When the delta is located at the shelf, the shelf and delta topset slopes are the same, however during periods when the delta left the shelf edge, only the angle of the delta topset is documented here.

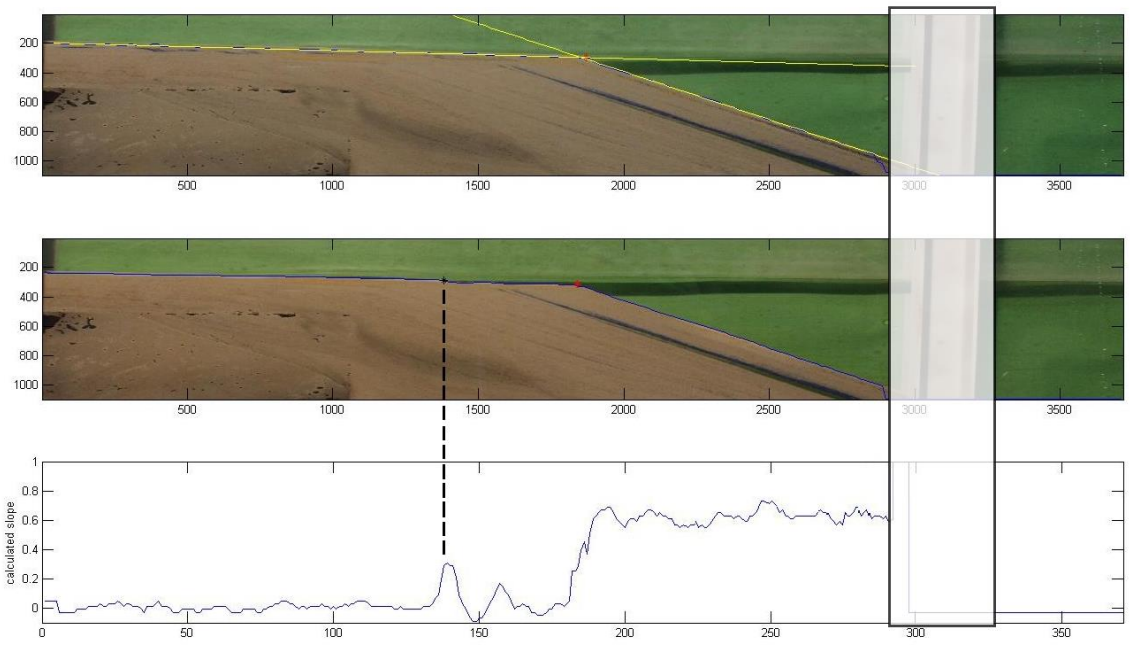

Figure 2. 5, Example of an analyzed photo in MATLAB. Upper panel (a) displays a photo with the delta located at the shelf edge. The yellow lines represent the linear fit lines used to determine the position of the shelf edge (red dot). The middle panel (b) shows a picture of the system in transgression, with the identified sediment surface (blue line), delta break (black dot) and shelf break (red dot). Lower panel (c) shows the calculated slopes that are used for identifying the delta break. The white bar hides a support beam of the flume, which makes it impossible to collect data in that area.

With these data points and values for every photo, the delta- and shelf edge trajectory and average topset slope through time can be documented for every experiment. Presenting a very detailed and easily comparable data set for the entire set of experiments.

2.4 Errors in the experiments and analysis.

2.4.1 Uncertainties during experiment.

The water enters the flume via an adjustable tap, which enables the addition of water to the flume to be controlled with a precision of 5 l/hr. The water pressure in the water supply system fluctuated, leading to a change in water discharge of approximately 5 l/hr. However, the water discharge was checked every 5 minutes, thereby keeping it as constant as possible. The sediment entered the flume via a calibrated screw feeder. The feeder can be set to the desired sediment flux with an accuracy of 90 ml /hr. The water outlet could be adjusted in height using a screwthread, the level of the water could be adjusted with an accuracy of 1 mm.

In the experiments that used a sea level curve, colored sand was added to mark the sea level high and lows (fig 2.5). To apply this colored sand the supply of sediment and water was halted. Furthermore, the colored sand has a different grain size. Adding the colored sand might have temporarily altered and influenced the mechanisms active in during the experiment. Additionally, the flow focused on one side of the flume, causing a small incision near the shelf edge. If this incision is located on the camera side of the flume a progradation rate slightly faster than average a larger topset angle might be measured. If

this incision is located on the other side of the flume the opposite effect might be possible. However, the duration of these episodes of focused or disturbed flow caused by the sand added seldom lasted longer than 5 minutes.

2.4.2 Uncertainties caused by the analysis.

During the MATLAB analysis, often the water surface was recognized in the photos, rather than the sediment surface. Additionally, the added colored sand and the shadow of the water surface are recognized as the sediment surface sometimes. This produces a noise in the smoothness of the sediment surface, which, in turn affects the averaged slope of the topset.

The greater part of these disturbances could be cancelled out by subtracting the values of the analyzed photo, from the photo that was taken 2.5 minutes later. Only the part in the photo that changed during this 2.5 minute interval, appears on the newly created image. Furthermore, the determined sediment surface was not allowed to deviate too far from the sediment surface in the previous photo, otherwise the data point from the previous photo was used. In cases where the scatter in the data points would remain extreme, the topset slope per photo would be calculated as the average topset slope of 5 photos. The average over 5 photos was taken because it covers 2.5 minutes. This is well below the time interval of 5 minutes, which is used to apply changes to the system. The noise that remains is approximately 0.01 fluctuation in topset slope and 2 cm fluctuation in shelf edge and delta progradation. The average topset per photo is used in the final figures.

The effect of the wrong surface being recognized as the sediment surface in the MATLAB analysis, is more extreme during periods of low topset slopes. This can be attributed to use of an average topset in the final result. An example of this effect can be recognized in figure 3.4, where the topset slope appears to have a negative value. This is however a processing effect.

Finally, the average slopes are plotted over time for all experiments. Since it concerns the average slope, concavity of the sediment surface is not taken into account here.

3. Results

3.1 Sea level experiments.

3.1.1 Comparison timing applied sea level change.

Figure 3.1 shows the location of both the delta and the shelf edge for the experiments developed to examine the effects of the increments of the applied sea level change (SL_HF_A1 and TR) (appendix 2). In this figure the given positions are relative to the location of the shelf edge at the beginning of the experiment and only the migration in the horizontal direction is projected. Transgression cycles can be recognized in this figure as the period where the delta- and shelf break curve don't coincide. In both experiments, two transgression cycles can be recognized. In between these cycles, both runs follow almost identical curves. The first transgression can be recognized during the first 20 minutes of the experiments, where the delta migrates approximately 20 cm landward in both experiments. Clear differences between the two curves can be seen during the second and better developed transgression episode. The curve of SL_HF_A1 is less smooth and the delta break moves approximately 8cm further landward during the transgression, the total landward migration for SL_HF_A1 is 24 cm. The SL_HF_A1 experiment is already 15 cm in transgression, at the start of the transgression in the TR experiment, 5 minutes later. Furthermore, the transgression in SL_HF_A1 appears to last about 7 minutes longer than in the TR run, to a total duration of 35 min.

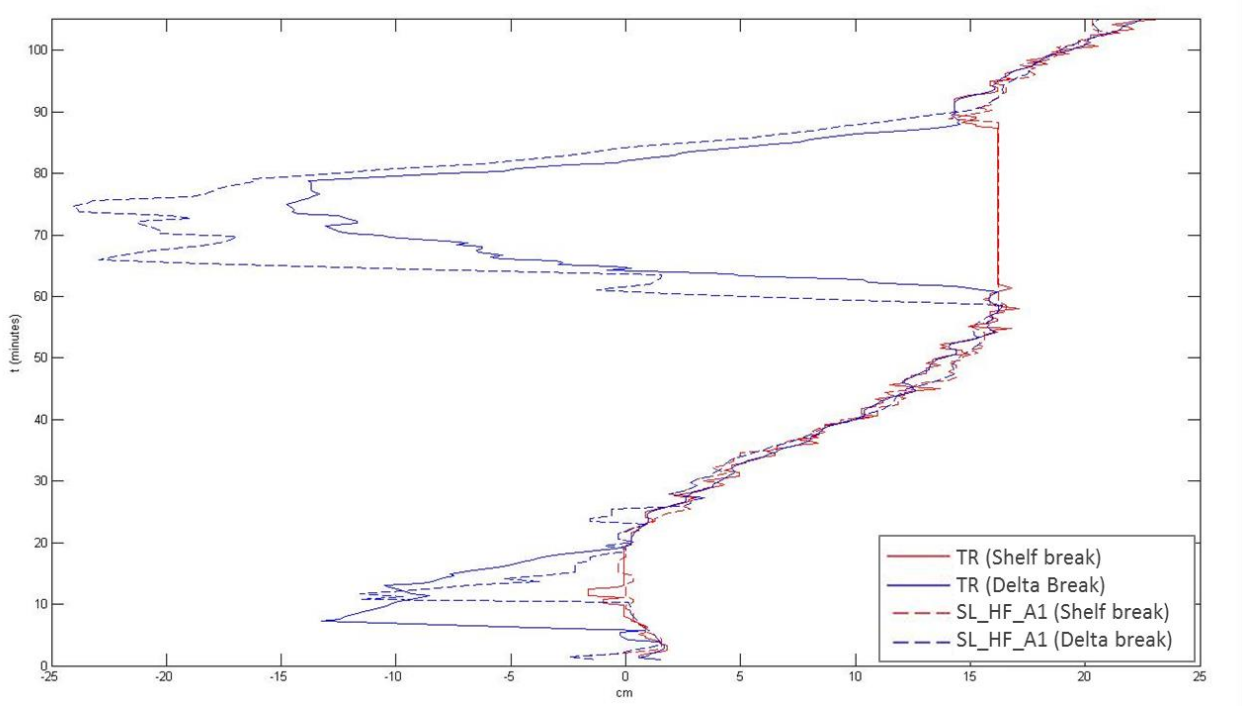

figure 3. 1, Delta and shelf break trajectories of the SL_HF_A1 and TR experiments.

Figure 3.2 shows the average topset slope over time for both experiments. The curve given in this figure represents the top set slope of the delta. These curves also show very similar trends. During the periods of high sea level the top set slopes are low, approximately 0.02, and during sea level lowstand the topset

slopes are slightly above the expected equilibrium slope of 0.04, indicated with the green dotted line (fig 3.2). Furthermore, during sea level lowstand the topset slope curve appears to level off and become constant for approximately 20 minutes in both experiments. The only difference between the two curves is the onset of the topset slope degradation, which starts approximately 5 minutes earlier in SL_HF_A1. This short time lag marks the beginning of the transgression can also be noted in figure 3.1.

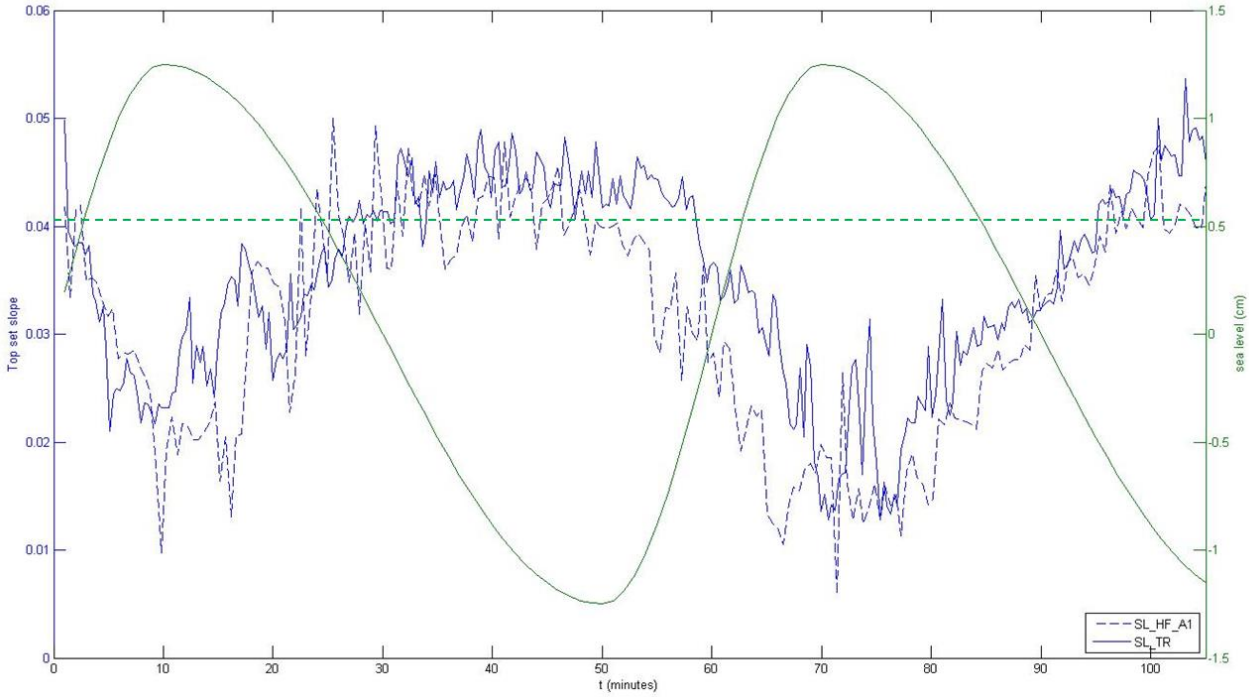

figure 3. 2, Calculated average top set slope over time for the SL_HF_A1 and TR experiments. The green curve represents the applied sea level curve, the green dotted line indicates the expected equilibrium slope.

3.1.2 High frequency sea level change with and without subsidence.

The delta and shelf break trajectories of high frequency runs SL_HF_A1 and SL_HF_A3 are represented in figure 3.3. Experiment names ending with A3 indicate that a sea level curve with subsidence was used (appendix 2). Both the delta and the shelf edge follow a similar path for the experiments. The most obvious difference is the amount of progradation of the entire shelf system. In the case where no subsidence is simulated, the shelf system progrades approximately 42 cm, whereas in the case with subsidence, the system progradates about 25 cm. Both experiments show 3 major transgression cycles where the delta leaves the shelf edge, a minor transgression event at the beginning and end of the experiment, where the maximal transgression is only 10 cm and the delta often reaches the shelf edge again within 5 minutes. A time period that coincides with the interval on which the sea level changes were applied. The duration and timing of the intervals at which the system is in transgression are comparable, however the distance of migration the delta experiences is different for the two experiments. The different distances transgressed by the deltas in the experiment are represented in table 3.1.

Although the distance increases in both experiments, it doesn't follow a clear trend. The transgression is 10 to 8 cm larger during SL_HF_A1 than SL_HF_A3, in the first and last cycle respectively. However they are equal during the second cycle.

transgression cycle	SL_HF_A1	SL_HF_A3
1	40 cm	30 cm
2	38 cm	38 cm
3	46 cm	38 cm

table3. 1, Distances migrated by the delta in SL_HF_A1 and SL_HF_A3.

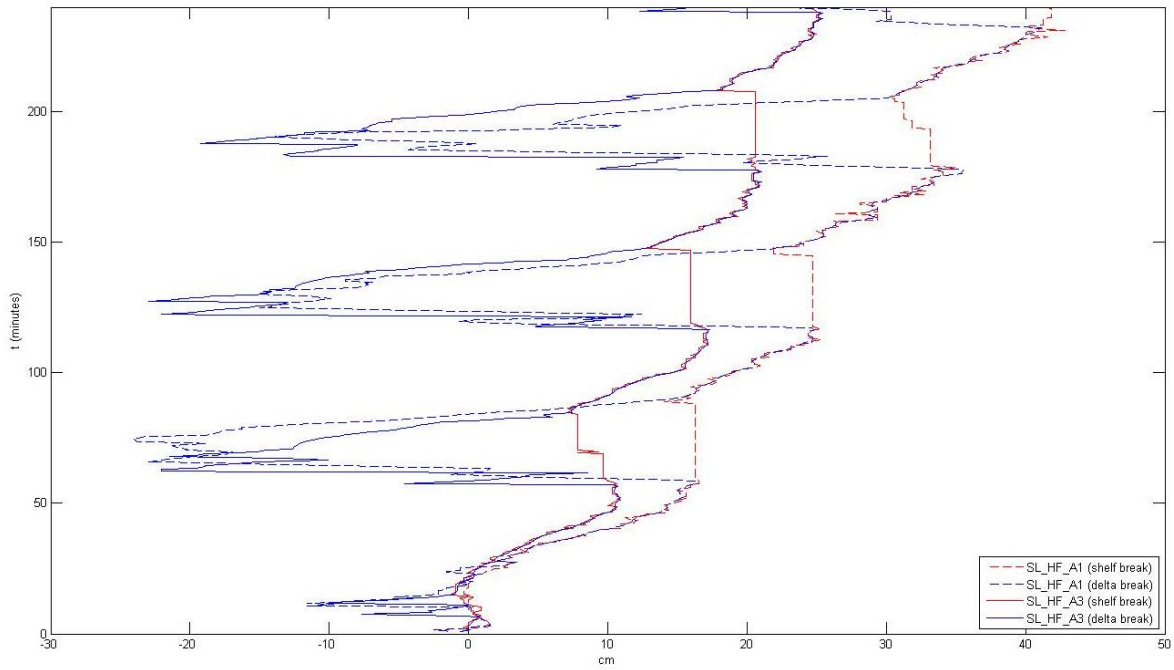

figure 3. 3, Delta and shelf break trajectories of the SL_HF_A1 and SL_HF_A3 experiment.

The topset slopes of both experiments also show a very comparable trend (fig 3.4). The minimum slopes are reached during the sea level high stand in both cases and are approximately 0.015. The maximum slopes developed during the seal level lowstand and are slightly higher then 0.04, which is comparible with the expected equilibrium slope for the sediment supply used in these experiments (0.04, appendix A). The peak in topset slope is located slightly before the lowest point in the sea level curve. During the third sea level cycle the trend in topset slope changes for experiment SL_HF_A3, however during the third cycle both curves coincide again. Note that the maximum slope that is reached during the experiment appears to lower from 0.045 to 0.038.

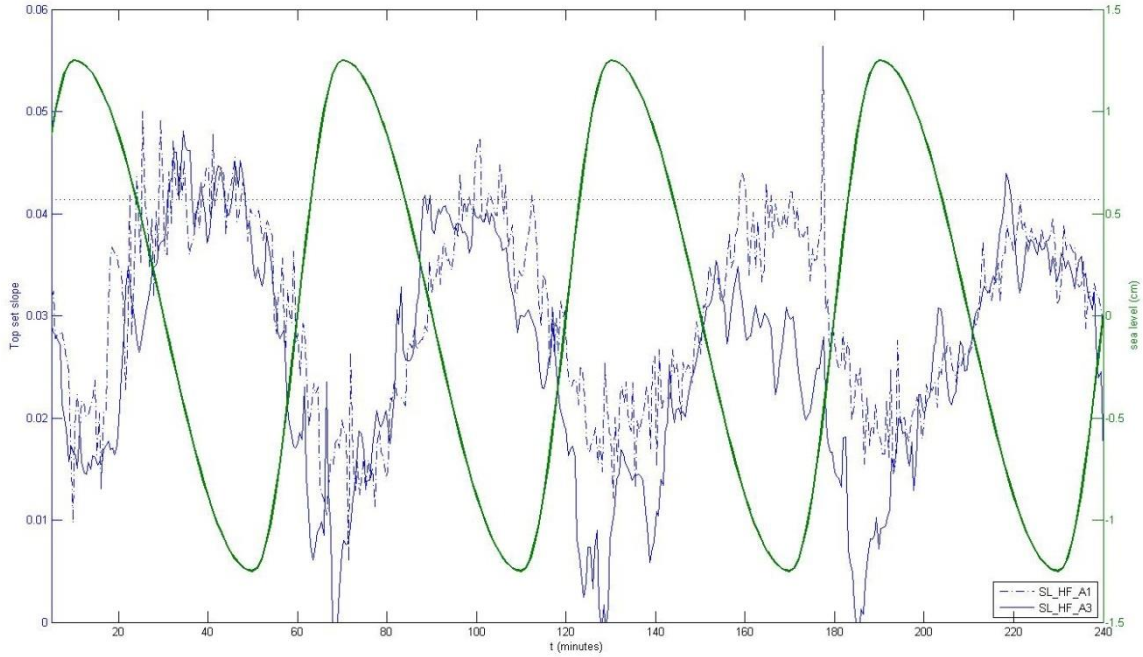

figure 3. 4, Calculated average top set slope over time for the SL_HF_A1 and SL_HF_A3 experiments. The green curve represents the sea level curve applied in SL_HF_A1. The sea level curve applied in SL_HF_A3 is the same, only with an added linear subsidence component of 4 cm over 4 hour. The negative angles of the topset slope during SL_HF_A3 are caused by the Matlab analysis, the analysis is more sensitive to disturbances caused by the water surface during periods of low overall topset slopes (chapter 2).

3.1.3 Low frequency sea level curve.

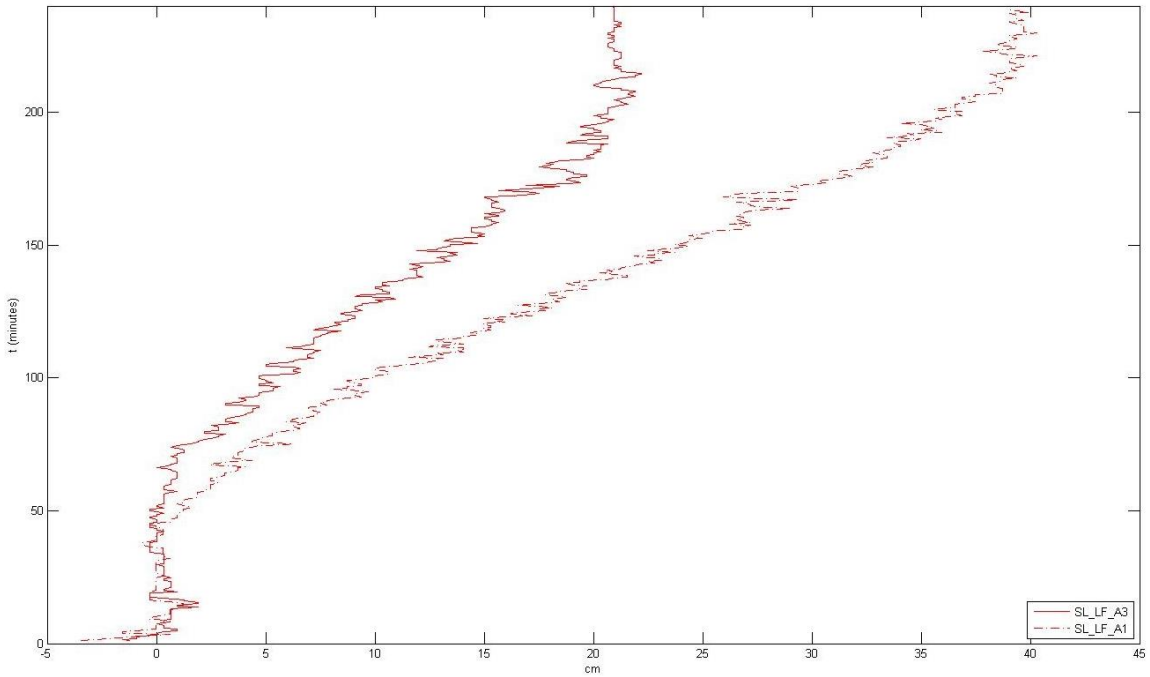

figure 3. 5, Shelf break trajectories of the SL_LF_A1 and SL_LF_A3 experiments. Because the system did not experience any transgression the shelf break paths are considered the same as the delta trajectories.

The system doesn't experience transgression, in any of the low frequency runs (fig. 3.5). The shelf edge trajectories in figure 3.5 represent the shelf edge trajectory of SL_LF_A1 and SL_LF_A3. The experiment ending on A3 indicates a sea level curve with a simulated subsidence of 1 cm/hr (appendix 2). During sea level rise both trajectories show periods of pure aggradation, depicted as a prolonged period of constant shelf break position during sea level rise. However, the delta never leaves the shelf edge. After 60 minutes, during the sea level fall they both show a linear progradation, until the next sea level rise. The obvious major difference is the final progradation, 21 cm in run SL_LF_A3 and almost 40 cm in run SL_LF_A1. Note that these values are almost identical to the values for the high frequency experiments. The topset slopes represented in figure 3.6 fluctuate in the beginning of the experiment, and are small, 0.015, during the period of high sea level. During the sea level fall, the slope increases until approximately 90 min, were both SL_LF_A1 and SL_LF_A3 become constant at 0.033 and 0.036 respectively. These constant slopes are slightly below the equilibrium slope. The maximum slope reached in experiment SL_LF_A1 starts to decrease again earlier than the slope in SL_LF_A3.

The results of the high and low frequency sea level changes, display differences in maximal slopes. The maximal slope reached during the high frequency experiments is slightly above the expected equilibrium slope. However, during the low frequency experiments the top set slope never reaches 0.04 and stays well below the equilibrium value at all times (fig 3.6). The minimum slopes however, are almost identical for these two experiments, namely approximately 0.015.

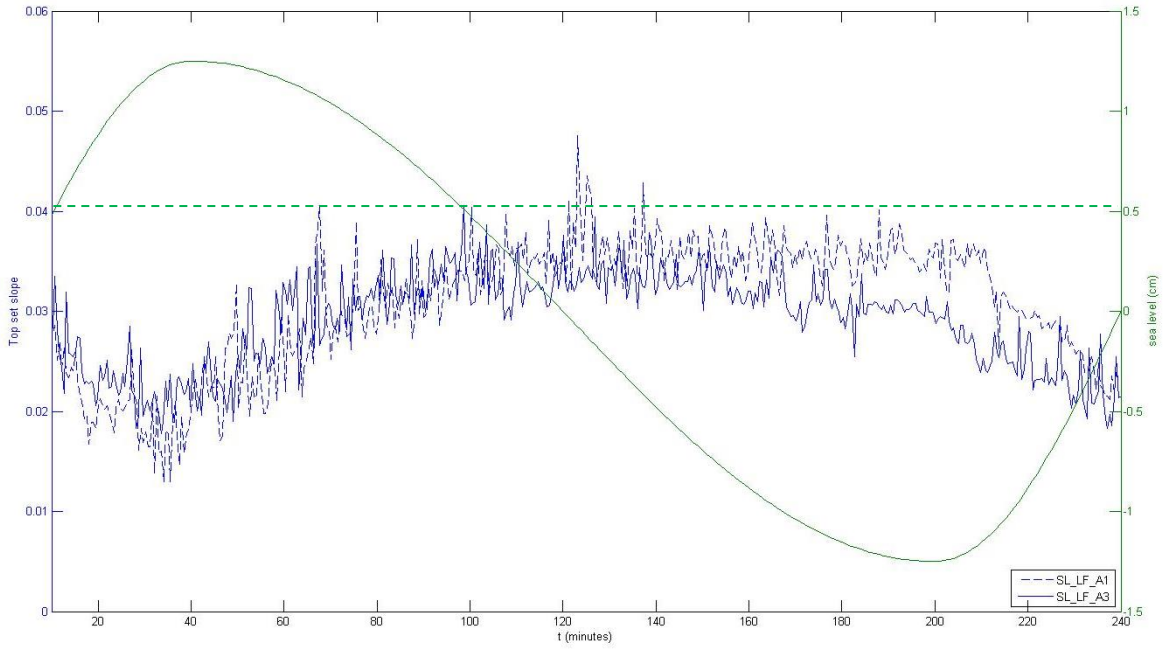

figure3.6, Calculated average top set slope over time for the SL_LF_A1 and SL_LF_A3 experiments. The green curve represents the applied sea level curve for experiment A1. The supply curve that was used in SL_HF_A3 is similar, however contains a subsidence component of 4 cm over 4 hours, thereby intensifying the sea level rise and weakening the sea level fall.

3.2 Sediment supply experiments.

3.2.1High frequency sediment supply changes.

The topset slopes measured during the sediment supply fluctuations show minimum values during low sediment supply and larger values during high sediment supply (fig 3.7). The amplitude of the fluctuations that can be observed is approximately 2.5 times smaller, in these experiments than in the sea level experiments, with a maximum amplitude of 0.01. During QS_HF_A1, the system experienced a fast increase in sediment supply and slow decrease (fig 3.7a). The calculated top set slopes fluctuate around the expected average equilibrium slope with an amplitude op approximately 0.005. The slope curve follows a much more symmetrical curve than the applied asymmetric sediment supply. There is a time lag between the peaks in the applied curve and the slope curve of approximately 20 minutes at the high and 10 minutes at the lows. The bottom panel shows experiment QS_HF_A7 (fig 3.7b), which experienced a slow increase in sediment supply and fast decrease (appendix 2), the calculated slopes follow the applied sediment curve without any clear time lag. The slopes appear to fluctuate around an average higher than the expected equilibrium curve, i.e. 0.044. After 90 minutes the slope stops fluctuating and becomes constant at 0.041.

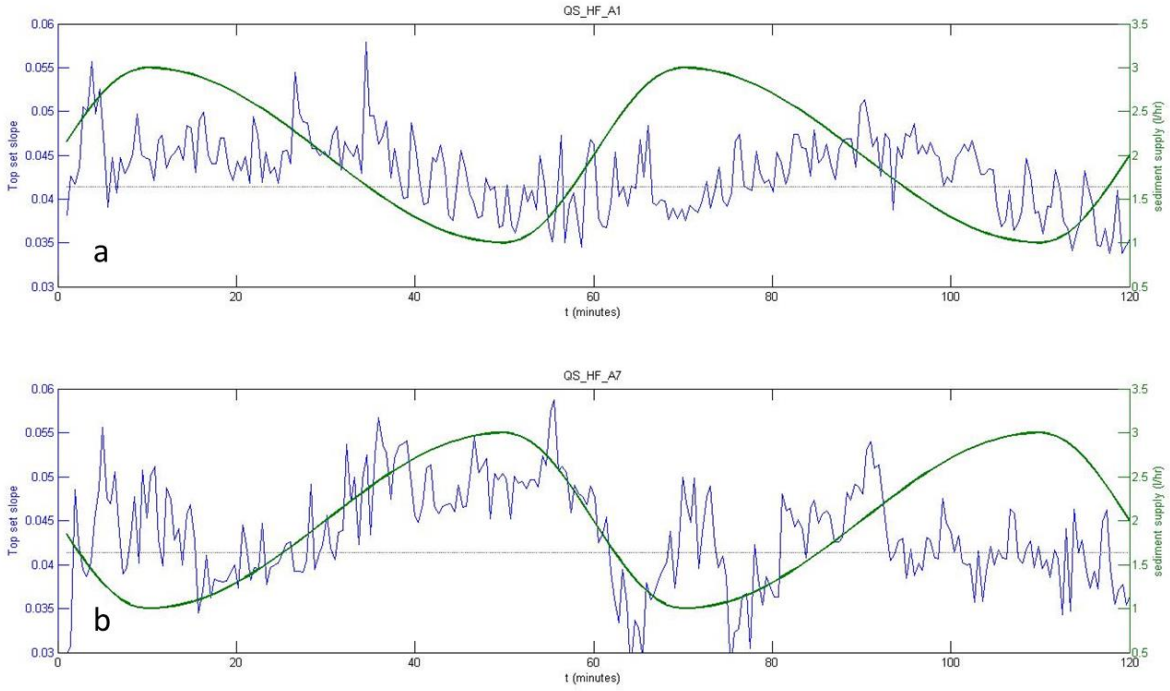

Figure 3.7 a. Calculated average top set slope over time for the QS_HF_A1, the green curve represents the applied sediment distribution curve. b. Calculated average top set slope over time for the QS_HF_A7, the green curve represents the applied sediment distribution curve.

3.2.2 Low frequency sediment supply changes.

During the low frequency sediment supply changes the top set slopes follows the sediment supply curve very nicely with a time lag of approximately 10 min (fig 3.8). After reaching the minimum and maximum slope during both the low and high sediment supply period, respectively, the slope remains constant for approximately 35 minutes. Note that the values fluctuate around the expected equilibrium value of 0.041, as one would expect (fig. 3.8). The variability of the signal increases after 170 min. This is thought to be an artifact of the analysis. Constant progradation of the system causes the shelf break to be located behind a support beam of the flume (fig 2.6), thereby hindering the MATLAB analysis.

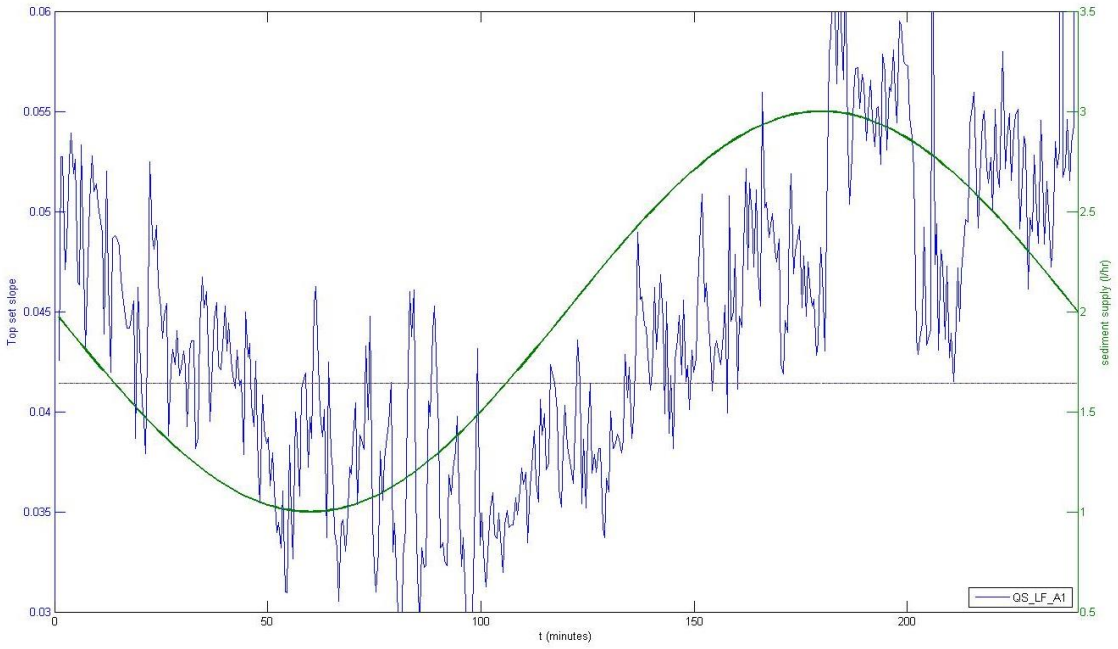

Figure 3.8, Calculated average top set slope over time for the QS_LF_A1 experiment. The green curve represents the applied sediment distribution curve.

Since no sea level change was applied during the QS experiments, the system did not experience any transgression.

3.3 Combined experiments.

3.3.1 High frequency sediment supply fluctuations.

During the combined experiments both the sea level and sediment supply fluctuates. In all experiments an asymmetrical high frequency sea level curve with a subsidence component of 1 cm/hr was applied. During C01_HF_A3 and C02_HF_A3 the sediment supply also fluctuated asymmetrical with a high frequency. In CO1_HF_A3 sediment apply increases fast and decreases slow and for C02_HF_A3 the sediment supply increases slow and decreases fast (appendix 2). During experiment C03_HF_A3 the sediment supply fluctuates with a low frequency symmetrical curve. In this section the results of the

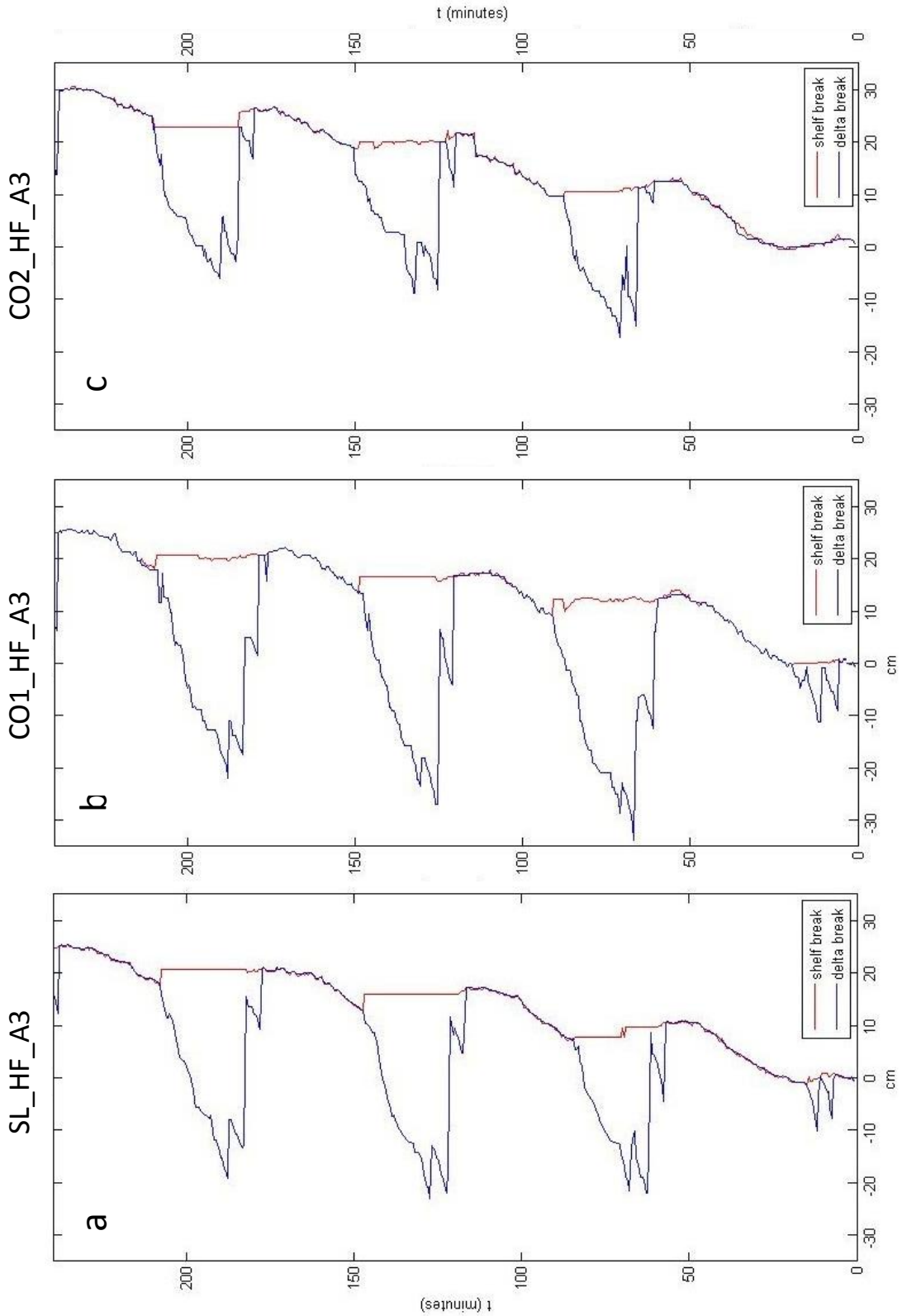

Figure 3.9, The delta and shelf break trajectories for the experiments SL_HF_A3, CO1_HF_A3 and CO2_HF_A3. Note how values of SL_HF_A3 appear to form an average of CO1_HF_A3 and CO2_HF_A3.

combined experiments are compared against the results of SL_HF_A3, where only the high frequency sea level curve with 1cm/hr artificial subsidence was applied.

When comparing the delta and shelf edge trajectories of SL_HF_A3, CO1_HF_A3 and C02_HF_A3 (figure 3.9), the curves of SL_HF_A3 and CO1_HF_A3 show very similar trajectories. SL_HF_A3 and CO1_HF_A3 have the same overall progradation, namely 25 cm. They both show three major transgression cycles and one minor transgression at the beginning of the experiment and the start of a fourth cycle near the end. The only clear difference, is the duration and extend of the transgression. Decrease in sediment supply during CO1_HF_A3 appears to have enabled the landward migration of the delta break by 6 cm (fig 3.9a). The average transgression in SL_HF_A3 is 36 cm and of CO1_HF_A3 is 43 cm. Furthermore, the transit time, the time needed to reach the shelf edge after the third and most extreme peak in transgression increased with approximately 5 min due to the applied sediment curve in CO1_HF_A3.

The trajectory of CO2_HF_A3 show 3 major transgression cycles (fig 3.9c). During the first episode of sea level rise, the delta did not leave the shelf edge at all. Every cycle shows a small transgression preceding the major transgression where the delta is able to transit back across the shelf to the shelf edge within the 5 min timeframe, in which the changes were applied. When this preceding transgression is included the duration of the cycles is of the same magnitude as the transgression cycles of SL_HF_A3. However, 5 minutes shorter that the transgression events in CO1_HF_A3. Also note that the transgressions of CO2_HF_A3 starts approximately 5 minutes later than the transgression in SL_HF_A1, even when the small transgression is included in the cycle (fig 3.9).

It is very clear that the lateral extend of the transgressions during CO2_HF_A3 is much smaller than the landward migration of the delta in SL_HF_A3 (36 cm) and CO1_HF_A3 (42cm) (fig 3.9). Landward extend of the transgression during CO2_HF_A3 is has an average of 28 cm landward migration. Please note, that the progradation of the shelf break is largest in CO2_HF_A3, namely 30 cm (3.9).

The calculated top set slope of CO1_HF_A3 (fig 3.10 a) and CO2_HF_A3 (3.10b) are compared to the topset slope of SL_HF_A3 (3.10). The curves of SL_HF_A3 and CO1_HF_A3 follow almost similar trends, with very close timing of the peaks and lows in the curves, as well as similar maximum and minimum slope values. The curve that describes CO2_HF_A3 shows overall higher values both during the lows and the highs. Furthermore, the time needed to reach maximum slope and the period of large slope values appear to last slightly longer. Also the timing of CO2_HF_A3 appears to reflect the sea level curve better than the other two curves, where the maximum and minimum slope values appear to fall slightly before the sea level extremes. Finally, the overall decrease in top set slope witnessed in curves CO1_HF_A3 as well as SL_HF_A1, cannot be found in the CO2_HF_A3 curve (fig 3.10).

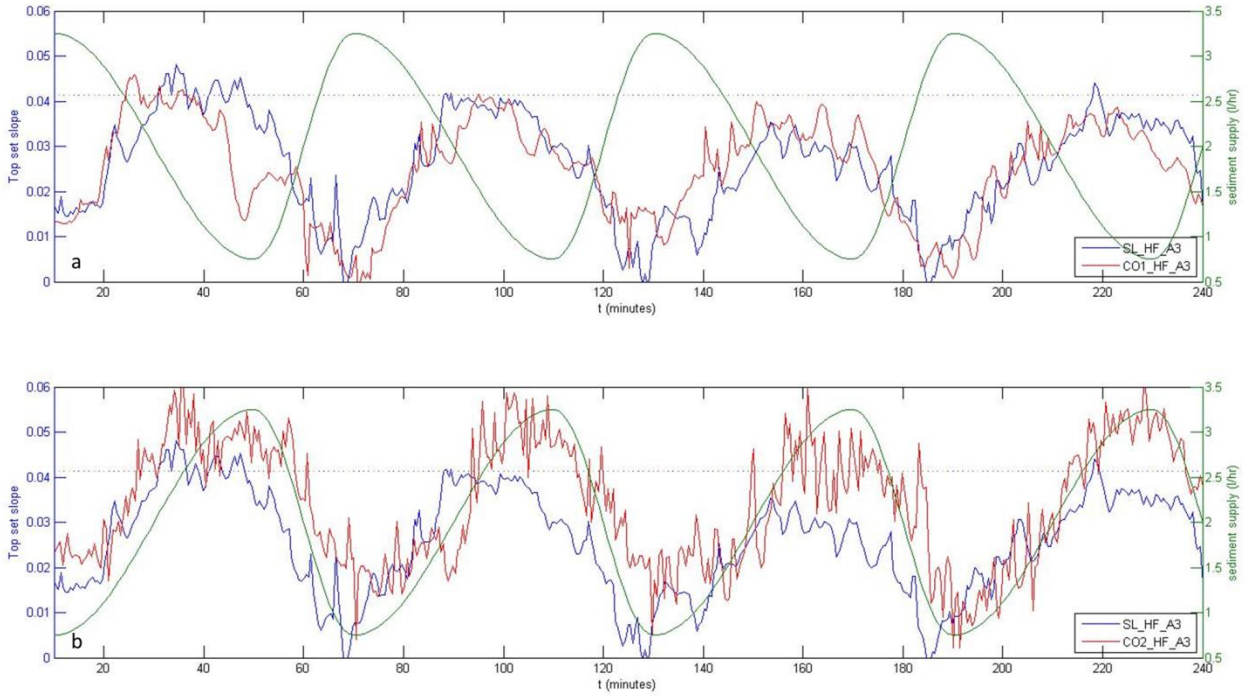

Figure 3.10 a, Calculated average top set slope over time for CO1_HF_A3 and b calculated average top set slope over time for CO2_HF_A3. The green curve represents the applied sediment supply curve, the blue line represents the calculated topset slope for SL_HF_A3 and the dotted line indicates the expected equilibrium slope from appendix 1.

3.3.2 Low frequency sediment supply fluctuation.

Figure 3.11 shows the delta and shelf edge trajectory for both SL_HF_A3 and CO3_HF_A3. Although the final position of the shelf edge is the same, and the trajectories follow similar paths, there are a few clear differences that can be noticed. First, the overall progradation pattern followed by the SL curve is uniform, whereas the shelf of experiment CO3 shows a slow progradation during the first part of the experiment, followed by fast progradation during the final part. Furthermore, during the first part of the experiment, when the sediment supply is low, the delta transgresses much further than during the second part with high sediment supply, 57 cm vs 20 cm respectively. The duration of the transgressions during SL_HF_A3 are approximately the same, i.e.25 min. Whereas the duration of the first transgression in CO3_HF_A3 is almost 50% longer than the third. During the first transgression cycle in CO3_HF_A3, the delta transgression was high enough for the delta to leave the photo twice, which is represented in this graph as the -50 cm point. Please note, that the length of delta migration during individual peaks within each transgression cycle are different. The general amount of transgression in between the changes applied every 5 min, for SL_HF_A3 is 10 cm, whereas the migration during the individual peaks in the first transgression cycle of CO3_HF_A3 is more than 11 cm and the maximum instantaneous migration during the last cycle is approximately 8 cm.

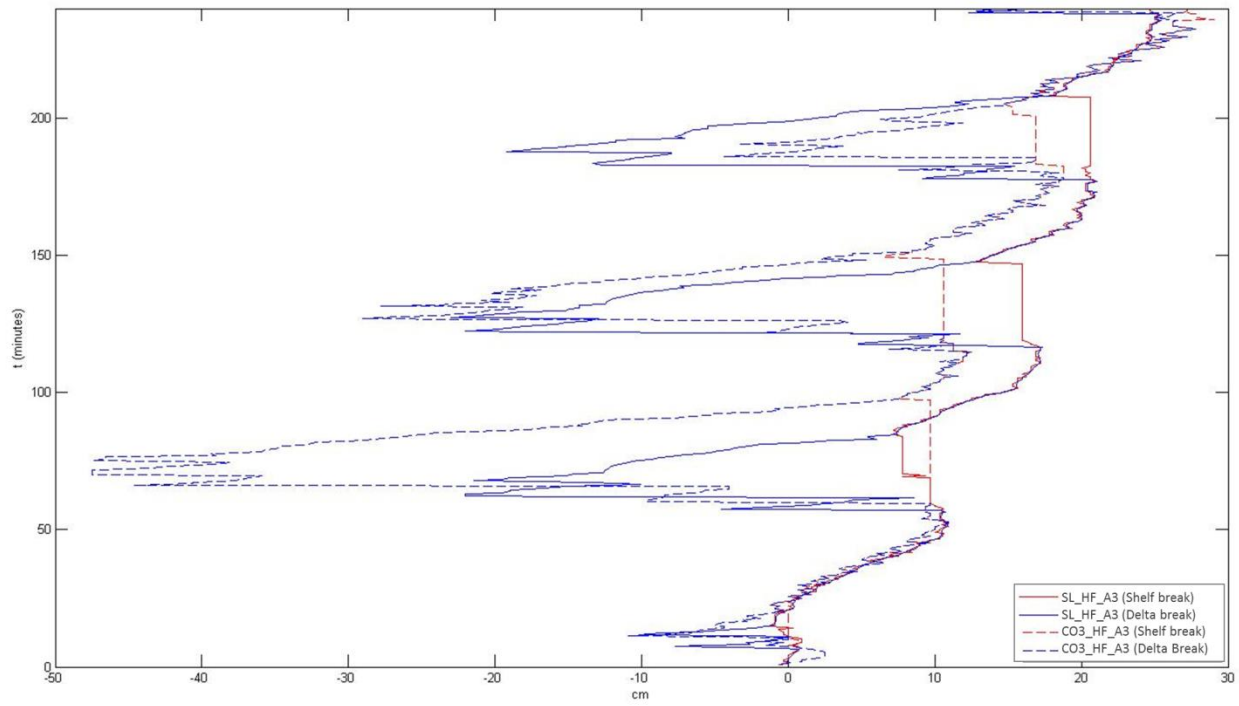

figure3. 11, Delta and shelf break trajectories of SL_HF_A3 and CO3_HF_A3. During the first transgression cycle, the delta migrates out of the picture. This can be recognized in the figure by the constant position at -48 cm.

When comparing the topset slopes (figure 3.12) of SL_HF_A3 and CO3_HF_A3, it is clear that even though there is a very clear high frequency noticeable in the CO3 experiment, a second larger frequency that coincides with the applied sediment supply curve can also be noticed. During the periods of lower sediment supply, the measured topset slope is approximately 0.015 lower than during the same time in experiment SL_HF_A3. However, during the period with larger sediment supply the two curves almost totally coincide. Around the 80 minute point the curve shows an extreme peak in topset slope.

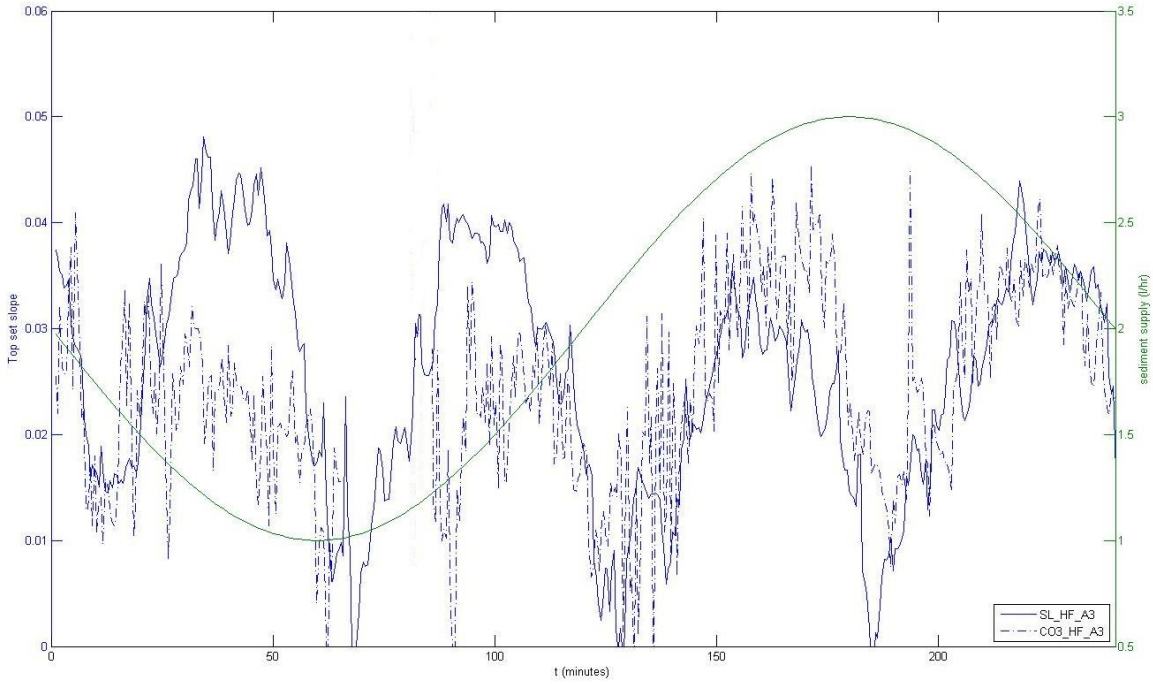

Figure 3.12, Calculated average top set slope over time for the SL_HF_A3 and CO3_HF_A3 experiments. The green curve represents the applied sediment supply curve. Between 65 and 90 minutes, an error during the photo analysis made it impossible to calculate the average topset slope for experiment CO3_HF_A3. The apparent negative angels of the topset slopes are artifacts created by the identification of the water surface as sediment surface during MATLAB analysis.

The last photo taken during SL_HF_A3 and the 3 combined experiments are represented in figure 3.13. The colored sand that was added during the experiments provides a clear marker of the preservation potential on the topset, during different combinations of sea level and sediment supply curves. In all four experiments represented in this figure, both blue, sea level highstand, and yellow sand, sea level lowstand, were added four times. Overall, preservation of the yellow sand on the topset is better in the sea ward end of the system. Only during the first two sea level cycles of CO3_HF_A3 experiment, the entire deposit of yellow sand is preserved. This indicates that no erosion took place on the topset, during sea level rise in those two sea level cycles. The worst preservation of the yellow sand is during CO1_HF_A3, when little to no yellow sand has been preserved on the topset. Preservation of blue sand on the topset, indicates low erosion during sea level fall. . Please note, that all experiments end during transgression and the fifth layer of blue sand has not been added in any of the experiments. The preservation potential of the blue sand on the topset increases during the course of PS_HF_A3. The blue sand deposited during the first cycle is completely removed, however, the sand added during the third sea level high is preserved over a large range of the topset. A notable difference can be seen between CO1 and CO2, where the preservation of the blue sand appear to take place in opposite ranges of the topset. In CO1_HF_A3 all blue sand that is preserved is located on the sea ward reach of the topset and vice versa in CO2_HF_A3. Last, the blue marker that was added during the first cycle in CO3 is completely preserved, whereas the blue sand added during the last cycle of the experiment is removed completely.

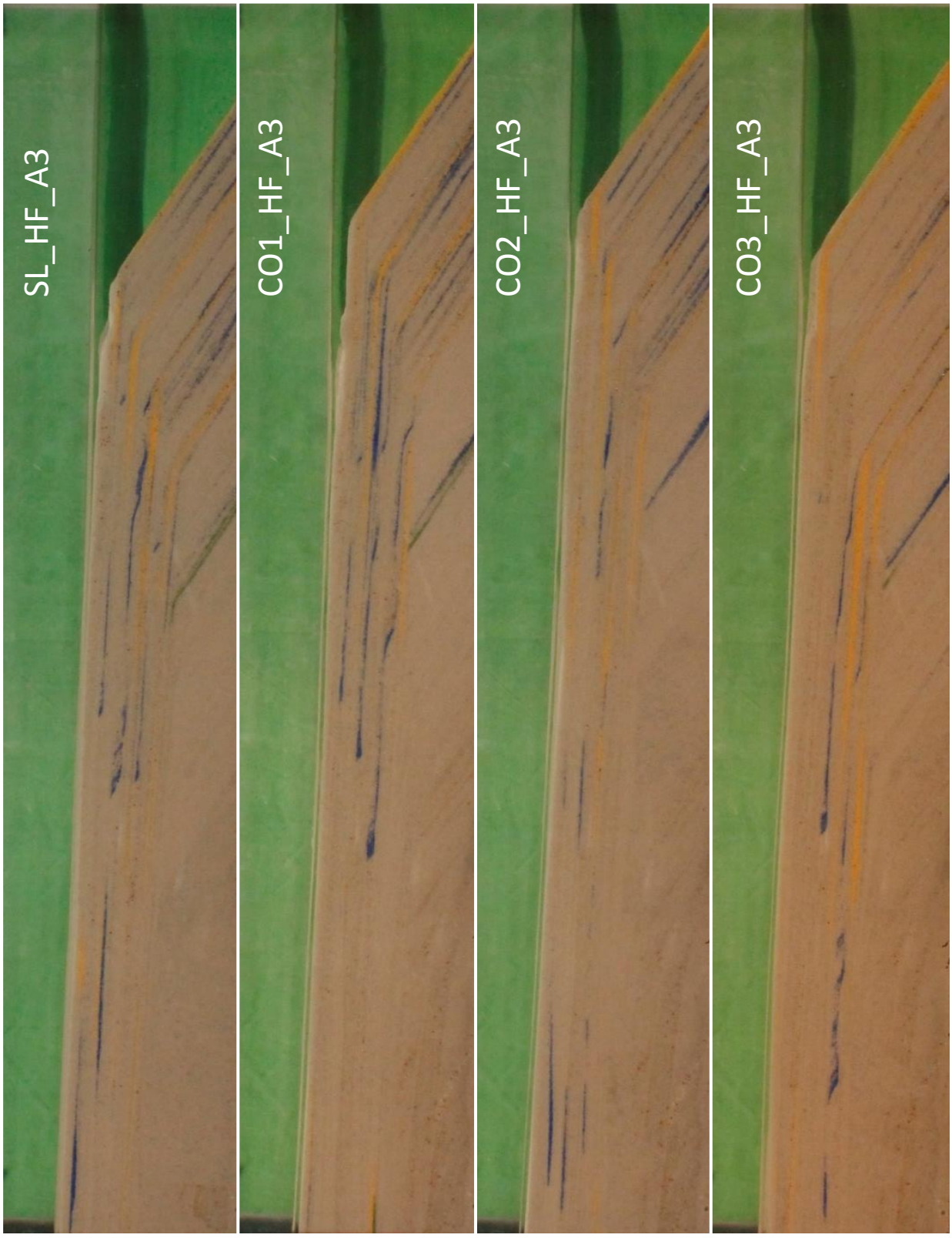

Figure 3.13, From top to bottom panel photos taken at the end of the experiments for SL_HF_A3, CO1_HF_A3, CO2_HF_A3 and CO3_HF_A3. The green sand was added before the start of the experiment, the blue sand during sea level highstand and the yellow sand during sea level low.

4. Discussion

4.1 Interpretations of results.

4.1.1 Timing applied changes in sea level.

The same sea level curve was used in the SL_HF_A1 and TR runs (Appendix 2), only the interval between applied changes was different. Shoreline trajectories and topset slopes were comparable for both runs, with two major differences. First, the TR trajectory curves showed smoother profiles than the SL_HF_A1 curves, especially during transgression. Secondly, the transgression during SL_HF_A1 lasted longer and the delta migrated further landward (fig 2.1). The longer time intervals constitute larger instantaneous changes. The system is knocked further out of equilibrium and the changes can be documented in the record, resulting in a less smooth curve.

With equal sediment supply, one would expect TR to be a smoothed curve of SL_HF_A1 with no major differences in absolute value. However, the delta transgresses further in SL_HF_A1 and it takes longer to reach the shelf edge again (fig 2.1). This can also be related to the system being knocked out of equilibrium by the larger instantaneous changes. The equilibrium slope of a system is relative steep and straight. A slope that approached an equilibrium profile is concave and less steep (Postma et al. (2008)). The same sea level rise would therefore be capable of migrating further landward, creating further transgression (fig 4.1).Furthermore, accommodation space create by the same sea level rise is smaller in a system with a steep, straight slope (fig 4.1), and more sediment and time is needed to fill the created accommodation space.

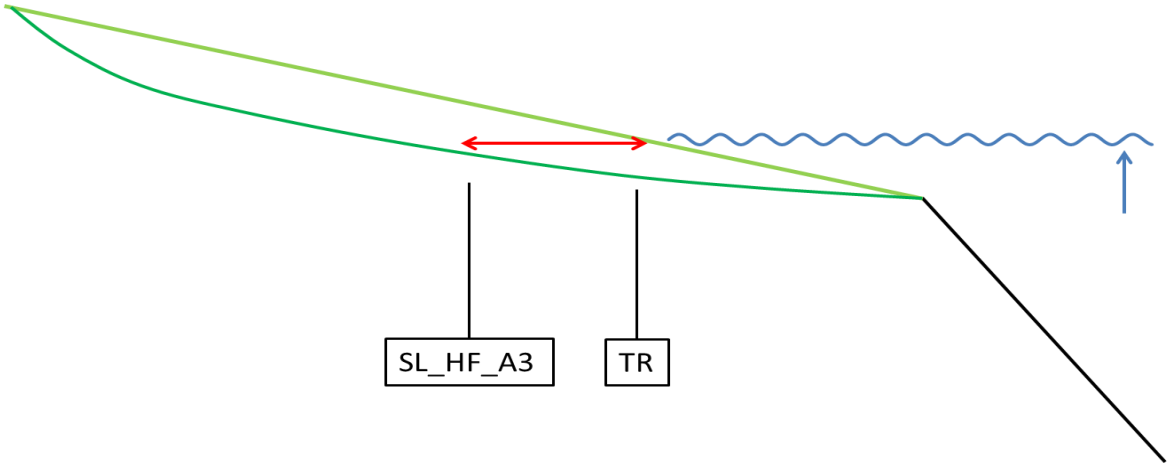

Figure 4.1, Schematic representation of a two different shelf topset slopes. The light green profile indicates a system that is in equilibrium, with a steep straight profile. The drak green line indicates a shelf building an equilibrium slope, resulting in a shallow, concave profile. The red arrow indicates the difference in landward migration of the shoreline during transgression.

The differences created by the different time intervals of applied changes appear to be small and well understood. Additionally, the 5 minute interval provides a very high frequency disturbance in the system that can be regarded parasequences.

The equilibrium slope is the stable slope of a system, were all sediment is bypassed (Postma et al, 2008). A depositional system is marked by a slope smaller than the equilibrium slope of the system and an erosional system will have a higher slope. The curves describing the three high frequency experiments display this mechanism very neatly. During sea level fall, a period characterized by erosion, the slope increases to high values. During the first and second sea level fall in the experiment, values exceed the equilibrium slope. This indicates that the topset was erosional during these periods. During sea level rise, the topset slope decreases, thereby indicating that the system is depositional and aggradation and sedimentation on the topset is possible.

4.1.2 High frequency sea level change with and without subsidence.

Due to the subsidence component, SL_HF_A3 experiences a larger sea level rise. The development of a larger accommodation space, due to the larger sea level rise, over the same sediment supply, would intuitively lead one to expect SL_HF_A3 to be more prone to transgression. However, the landward migration during transgression in experiment SL_HF_A1 is 10 – 15 cm larger than in SL_HF_A3 (fig 3.3). This counter intuitive result can be explained by considering the shape of the sediment surface. During progradation a concave surface develops with the horizontal part located at the sea ward end of the surface (fig 4.1). Faster progradation increases the concavity of the surface. Since SL_HF_A1 doesn't have an overall aggradational component, it progradates 1.7 times faster than SL_HF_A3. The increased concavity created by this faster progradation, enables a larger landward migration of the sea during sea level rise, and therefore leads to larger transgression.

In the SL_HF_A1 run, the entire system is progradational and only a very small component of the supplied sediment is stored in the topset. In SL_HF_A3 a subsidence component was added to the sea level curve (appendix 2), this causes the system have an aggradational component. Consequently, the system can store sediment in the topset and thereby hindering the deposition of sediment on the foreset. The same average topset angles are developed in both experiments.

SL_HF_A1, SL_HF_A3 and TR all show a steep topset slope during sea level lowstand, caused by the erosive nature of the system and a shallow slope during sea level high stand, marking a depositional system. During the course of the experiment the maximally reached topset slope decreases (fig 3.4). This can be attributed to two mechanisms. Both consider the length scale of the system. Since the equilibrium time is quadratic proportional to the length scale (Paola et al. (1992)), an increase of approximately $\sqrt{2}$ (progradation from 1m to 1.42m) would double the equilibrium time. Although the frequency of the applied sea level change remains constant during the entire experiment, the progradation of the system doubled the equilibrium time. Hence, the period of the applied changes shortens relatively to the system and it can no longer develop its equilibrium slope. The maximum reached slope decreases. The other explanation includes the concavity of the slope. Since only the averaged topsets are considered in the results, increasing the concavity of the surface would result in a lowering of the average value. An increased equilibrium time would increase the time needed to develop a straight slope and thus resulting in development of a smaller slope.

The average topset slopes in both experiments are equal, except for the third cycle of sea level fall. Here, the SL_HF_A3 show lower values for the calculated slope. This is attributed to an error in the MATLAB analysis. Supposedly, a previous transgressive surface marked by colored sand was measured instead of the newly formed one.

4.1.3 Low frequency sea level curve.

The effect of a low frequency sea level curve was tested during SL_LF_A1 and SL_LF_A3, where the latter experienced a subsidence component (appendix 2). The sea level fluctuations on the long time scale produce no transgression (fig 3.5). This indicates that at the magnitude of fluctuation the system is able to adjust its boundary conditions without severely changing its shape. After an initial period of dominantly aggradation, due to sea level rise, both experiments show a linear shelf edge trajectory.

After approximately the same period, 90 min, during which the top set slope fluctuates, the topset slope also becomes constant (fig 3.6). The angles developed are slightly lower than the equilibrium slope, this is caused progradation and aggradation on the topset. Progradation causes constant lengthening of the system, which prevents the equilibrium slope to be reached. However, since the parameters describing the system are constant, the system can still be described as in equilibrium. The subsidence component added to the SL_LF_A3 experiment decreases the rate of sea level fall thereby decreasing progradation rate and thus increasing the developed equilibrium slope. Furthermore, the lowering of the developed slope in SL_HF_A3, before the start of the sea level rise (fig 3.6), indicates that the lengthening of the system destabilizes the equilibrium state.

During the third and fourth high topset slope period in experiments SL_HF_A1 and SL_HF_A3 the maximum slopes remain below the equilibrium value. This could indicate that the system is depositional during periods of sea level fall. However, the low frequency experiment showed that the stable slope developed during sea level fall is slightly below the expected equilibrium slope. Therefore, one should not consider the equilibrium slope measured without progradation, when determining the depositional vs erosional nature of the system. Instead, to determine the nature of the system it should be compared to the slope developed under steady progradation at a known rate.

4.1.4 High frequency sediment supply fluctuations.

During equilibrium state all sediment that enters the system will be bypassed. To this purpose a system that receives more sediment, it will adopt a higher angle, in order to maintain the kinetic energy to transport all the sediment and vice versa. The basic effect of this mechanism can clearly be recognized in the sediment supply experiments, both high and low frequency. The asymmetry of the high frequency curves, create large differences between the two. The forming of the slope appears to need more time than the degradation of the slope. The sediment curve used in QS_HF_A1 has a rapid increase of sediment supply and a slow decrease (appendix 2). Since the period of aggradation during QS_HF_A1 are short, the maximum angles reached here are less than the maximum angles in QS_HF_A7 where double time was provided for the build up of the slope. Secondly the degradation of the developed slope appears to be much more instantaneous. Degradation only starts at the moment when the sediment supply is decreased below the value at which the developed slope is stable. Since the

maximum stable slope is never reached in QS_HF_A1, the degradation doesn't start at the same moment as the sediment supply decreases, but shows a time lag of 25 min. The combined effects explain why the slope development follows the sediment curve much better in QS_HF_A7.

The same mechanism can explain the fluctuation in slope angels during the low frequency sediment fluctuation. A low angle with low sediment supply and high angle with high sediment supply. The angle remains constant for 25 min at the minimum and maximum, indicating that the system has time to develop equilibrium. Note that it is not so clear equilibrium as in SL_LF_A3, so maybe different equilibrium times are applicable for different forcing mechanisms.

4.1.5 Combined experiments.

High frequency sediment supply fluctuations.

The delta and shelf break trajectories of the high frequency combined experiments have been compared to SL_HF_A3 (fig 3.9). In CO1_HF_A3 the transgression coincides with periods of high sediment supply, therefore one would expect less transgression. However, when compared to SL_HF_A3, during transgression the delta in CO1_HF_A3 migrates further landward. This implies that not the sediment supply, but the memory of the topset is the dominant factor in the nature of the transgression. When the delta is located at the shelf edge, Sl_HF_A3 and CO1_HF_A3 show very similar trends. Transgression is expected to be extreme in CO2_HF_A3, because it coincides with periods of low sediment supply. However, the landward migration during transgression in CO2_HF_A3 is very small. The high topset angle created in CO2_HF_A3, decreases the created accommodation space on the topset during a transgression cycle. The system is able to fill the accommodation space fast and decrease the duration and length scale of the transgression. In addition to the previous mentioned explanations, one should consider that the effect of sediment supply is stronger in the more proximal part of the system, i.e. outside of the photo analyzed in this report. Storage of sediment on the topset further upstream might cause a time lag in the effect of sediment supply on the system.

The amplitude of the measured fluctuations in topset slope caused by changing sea level and sediments supply are 0.015 and 0.005, respectively. The amplitude of the changes in topset slope in the combined experiments is 0.015. No difference in amplitude can be seen between SL_HF_A3, CO1_HF_A3 and CO2_HF_A3 (fig 3.10). SL_HF_A3 is used as a reference experiment here aswell. The absolute value and timing of topset development do show different values, when comparing the combined high frequency experiments with SL_HF_A3.

Sea level change and sediment supply have opposite effect on the system. Increase in sediment supply causes a steeper slope, sea level rise causes a decrease in slope. The most extreme effect of the applied changes in topset slope can be recognized during the experiment where both curves are in anti-phase (CO2_HF_A3), as expected. The average slope developed in the CO2_HF_A3 experiment is higher. During the CO2 experiment the assymetric character of the applied sediment supply curve creates longer time span to develop a larger slope. Furthermore the coincidence of the high sediment supply with the low sea level, requires a larger slope angel for the system to become erosional. Because of the shorter time to degrade the topset angle, this reinforcing effect has no time to develop during the sea

level rise. This explains the higher average topset angle and why the maximum angle is reached later during the sea level fall. The sediment supply has no measurable influence on the developed top set curve in CO1_HF_A3. This can be explained by two mechanisms. First, the measured effect of sea level fluctuations is 3 times stronger than the measured effect driven by the sediment supply. Secondly, the build up of the topset slope takes longer than the degradation. The fast increase in sediment supply (CO1_HF_A3) doesn't allow the development of the higher angles of the topset.

Changes in sea level affect the distal part of the system and migrate landward. Changes in sediment supply operate from the proximal part of the system and prograde seaward. The part of the system that is analyzed from the photos and considered in these experiments is, the distal part of the system. Therefor, the effect of sea level might be overestimated in this report with respect to the effect of sediment supply.

Low frequency sediment supply fluctuations.

The effect of the low frequency sediment supply curve is clear during the first half of the experiment, where it decreases topset angle during sea level high and a strong reduction in the maximum topset slope during sea level low (fig 3.12). In the second part of the experiment this effect can no longer be witnessed. During the beginning of CO3_HF_A3 the fluctuation in topset slope by changing the sea level is affected by the sediment supply effect. This causes an even lower topset angle during sea level high and a strong reduction in the maximum topset slope during sea level low. The effect of this interaction becomes clear in the delta and shelf edge migration graph. Due to the low topset angle, the shoreline is able to migrate further landward during the transgression and the created accommodation space is increased. The low sediment supply prevents fast progradation in between the applied sea level rises. This results in a much larger transgression on both time and space scales.

4.1.6 Preservation potential

Figure 3.14 shows how the interaction between the applied sediment supply curves and the used sea level curve, influences the preservation potential of different stratigraphic surfaces. Please recall that the yellow sand was added during sea level low. The lowstand deposits in all experiments are dominantly preserved in the distal part of the system. The blue sand, added during sea level high, is preserved in different parts of the system in the different experiments. The upper panel shows the deposits of SL_HF_A3, where only a sea level change was applied (appendix 2). Although the applied sea level changes remain the same during the experiment, different parts of the topset are being preserved. In the beginning of the experiment, the system is relative short and the blue sand is removed from the proximal part of the system. The apparent preservation of deposits in the more distal parts of the system, indicated by the presence of blue sand in this area, could also be caused by the reworking and redeposition of proximal deposits. During the third and fourth sea level cycles, the system is longer and the proximal sediments are preserved. This supports the assumption that base level fluctuations affect the distal part of the system and migrate upward from here. Furthermore, it illustrates again how the length scale of the system influences its behavior. The preservation of the reworked blue sand indicates

that erosion didn't continue long enough to remove all blue sand from the topset. Furthermore, it could also indicate that the erosion is focused in one area at one time.

When a sediment curve is added to the experiment, the preservation of highstand deposits changes. In experiment CO1_HF_A3, where the sediment and sea level curve are in phase, sediments from the proximal part of the topset are eroded (fig 3.13). This indicates erosion of the entire topset during sea level fall. However, the preservation of the reworked sediments on the distal end of the shelf, indicates that the erosional nature of the system didn't prevail for a long period. During experiment CO2_HF_A3, highstand sediments are preserved in the proximal part, indicating that erosion caused by base level fluctuation didn't reach the proximal part of the system. The increase in sediment supply during sea level fall, decreased the extend and duration of erosion. The system switched back to an overall depositional system faster.

During the first 2 sea level cycles of CO3_HF_A3 the blue sand is preserved at the distal part of the system, indicating that the erosional event stopped before the blue sand was completely removed from the topset. In the second half of the experiment, during low sediment supply the erosive system continued until the all blue sand was removed. The high topset angles caused by the increased sediment supply, stimulated erosion on the topset during sea level fall. Although it wasn't the initial intention of the research, the colored sand added to the experiments provide a good insight in the preservation potential of the system.

4.2 Implications for application of sedimentary models.

4.2.2 Time scales.

Different time scales become apparent when analyzing the results of the experiment. Three major time scales can be recognized, a. the 5 minute interval at which the changes are applied to the system. b. the high frequency changes with a period of one hour, which are thought to coincide with the equilibrium time. c. the long timescale of 4 times the equilibrium time. It becomes clear from the low frequency sea level experiments that every system has a time scale at which changes can be applied and a new equilibrium develops. i.e. the system is no longer sensitive to the applied changes. This timescale is determined by the boundary conditions of the system. Changing these boundary conditions changes the equilibrium time. For example, both experiments SL_LF_A1 and SL_LF_A3 reached a new equilibrium after 90 min, thereby demonstrating similar reaction to the applied change. However, in SL_HF_A1 the increasing length scale made it more vulnerable to change. Although the applied sea level change was smaller, the system got knocked out of its equilibrium state earlier in this experiment.

The changing time scales at which the system functions becomes very clear when looking at figure 3.4. During the first cycle the topset slope reaches its maximum 15 minutes after the first peak in sea level. It remains the same for approximately 20 min. After the second sea level maximum it reached the maximum slope again after 15 minutes, only it remains the same for only 10 minutes. The increase in length scale of approximately 10% (fig 3.3) already destabilized the equilibrium and made it more sensitive to allogenic forcing. With continuous lengthening of the system, the equilibrium value of the slope is not reached. This supports the theory that every system has one characteristic time scale at

which it is sensitive for changes (Paola et al, (1992) and Postma et al, (2008)). Changes in the bounding parameters of the system, will affect these time scales. Forcing applied on longer or shorter timescales will not be able to affect the system.

The sediment supply experiments show that the time needed to reach equilibrium after an increase in sediment supply is longer than the time needed after decreasing sediment supply. The rate of infill of created accommodation space is typically nonlinear (Postma et al. (2008)). In other words, the fill up rate to equilibrium decreases as the system approaches grade. Therefore, the system responds slow to the changes in sediment supply. This gives rise to the idea that a system has not one, but several characteristic time scales at which it operates. Each time scale directly associated with a different forcing mechanism.

Ordered time scales, which are often used in sequence stratigraphy, are often linked to allogenic factores, e.g. tectonics, eustacy and sediment supply. One could state that an ordered hierarchy of sequences is necessary, because of the superposition of cycles in the data. Unless detailed analysis indicates that a particular pattern arises from superposition of cycles of different periods, the presence of superposition is no direct evidence of hierarchy (Schlager (2009)). The present used hierarchy appears arbitrary, instead of a detailed process driven subdivision into orders of similar lengths. In their attempt to standardize sequence stratigraphy Catuneanu et al. (2006), propose a new scheme of orders which would lead to regional subdivision instead of global hierarchy. The new proposed first order cycle, covers the original first to third order ranks. Thereby indicating how arbitrary the commonly used ordered-hierarchy approach is. The result presented in this study indicates that time scales on which the system is affected are dominantly determined by the scale of the system, rather than the time scale of the applied changes. Again, advocating against the use of a set order hierarchy. When orders are determined, their duration and hierarchy should be determined by the physical parameters bounding the system.

4.2.2 Transit time.

Timing of location of the delta at the shelf edge has received a lot attention in recent years. In their experiment Muto and Steel (2008) have shown the shelf slope to be the dominant factor in determining whether the delta can reach the shelf edge during sea level rise or high stand. In the experiments presented in this report, the delta never reached the shelf break during sea level high stand. However, the present results do support the theory of shelf slope being the dominant driving factor. Although, sediment supply was high during transgression in CO1_HF_A3 and low during transgression in CO2_HF_A3, the landward migration during transgression was smallest during CO2_HF_A3. The high angle created during the period of high sediment supply, prevented base level to migrate landward during sea level rise. Thus creating less accommodation space and enabling the delta to migrate to the shelf edge faster.

4.2.3 Sequence stratigraphy, trajectory analysis and terminology.

Sequence stratigraphy is the most recent conceptual model to order stratigraphy and define a sedimentological model. It provides a good framework to determine the chronological order of basin fill

and stratal stacking patterns and their response to allogenic forcing, such as sediment supply and base level change (Catuneanu et al, (2009)). However, controversy remains in determining the most usefull surfaces for correlation and what surfaces should define a sequence boundary. The marine part of the maximum regressive surface combined with the subaerial unconformity, are used as the sequence boundaries to transgressive-regressive sequences. The sequence boundary to depositional sequence is formed by the subareal unconformity and its correlative conformities. Erosion might have been focused and not be recognizable on a regional scale. The boundary to a genetic stratigraphic sequence is formed by the maximum flooding surface. Maximum flooding surfaces are often easy to recognize in log, core and outcrop data (Catuneanu et al. (2006)), however, a detailed look into the experiment and its preservation potential shows that the maximum flooding surface is often been reworked. The maximum regressive surface and normal regressive systems tract are preserved in all experiments. Suggesting that in a dominantly sea level driven, simple shelf system the transgressive-regressive sequence approach might be most suitable.

An alternative approach to defining and describing a system, is using the shoreline and shelf edge trajectory (Helland and Hansen (2009) and Helland et al. (1996)). For the present experiments the trajectories of both the delta and the shelf edge can be followed easily due to the photo analysis. However, erosion of the shelf break and often a large part of the shelf topset, makes it difficult to observe trajectories and they can only be implied. Well-chosen stratigraphic surfaces require less interpretation and could lead to a more accurate analysis. Additional research in similar analogue flume settings, could greatly improve the understanding and predictability of preserved surfaces in sequence stratigraphic models.

4.3 Implications for real world sedimentary systems

4.3.1 Longitudinal profiles

In the literature various examples of delta systems, where a steep slope has developed during forced regression and a gentle slope during transgression or sea level high stand, can be found. Using seismic and core data for the Rhone delta, Berné et al (2007) clearly demonstrate the influence of sediment supply on the preservation of large sand bodies on the shelf, during deglaciation driven sea level rise. Their data suggests a difference in slope for the Messinian incised valley and the Quartnary transgressive deposits (fig 4.2a). Numerical modeling of fluvial profiles, taking into account the erosional en depositional features of the system, and comparison with the present day Rhone geometry, again, indicate steep profiles during sea level low (Loget 2006).

Bowman et al. (2007) examined how desert streams adjust to the rapid and continuous base level lowering in the Dead Sea, on short time scales of tens of years. Core analysis and field data enable to distinguish between the Dead Sea flat bed and fluvial channels. Longitudinal profiles of the entrenched channels show a larger slope than the fossil fan deltas, with a difference up to 4°(fig 4.2b). For the dessert streams it is suggested that the initial relief dictates the longitudinal transient profiles. Numerical modeling of the alluvial incision driven by the base level drop in the Dead Sea, predicts a continuous steepening of the longitudinal profiles in coming years (Moshe et al. (2008)).

The Holocene palaeogeographic evolution of the Rhine-Meuse delta has been extensively studied (Berendsen en Stouthamer (2001), Cohen (2003) and Hijma and Cohen (2011)). The gradient lines of the rivers have been established based on lithological borehole descriptions and dated archaeological sites (Berendsen en Stouthamer (2001)). Again, the difference in gradient between sea level fall and lowstand deposits and the slopes formed during sea level rise become apparent (fig 4.2c). The different gradients are attributed to Early Holocene temperature rise and restoration if the vegetation, which led to a decrease in peak discharge if rivers, a general decrease of sediment load and a relatively increased sediment load of fines (Berendsen (2005)). Tornqvist (2002) points out that the upstream convergence of river terraces in the Rhine-Meuse system cannot solely be explained by subsidence rates and proposes different grading of the river profiles controlled by both sediment supply and sea level rise.

Examination of the Lower Mississippi longitudinal channel profiles indicates that late Pleistocene braid belts have steeper gradients (fig 4.2d), than the modern Mississippi River (Rittenour (2007)). The difference in riverprofile between glacial and interglacial periods is contriburted to alvulsion cycles, preventing the channel to incise into older sediments, difference in water discharge and sediment load. It is assumed that the channel profile is controlled by the upstream forcing by sediment supply and water discharge and the basement profile and profile of the incised valley are controlled by eustatic sea level (Rittenour (2007)).

Additional examples show the same geometry. Studied river terraces of the Susquehanna River (Pennsylvania) show steeper terrace profiles during periods of sea level low (Pazzaglia and Gardner (1993)). The river valley fills by alluvial and estuarine deposits of the Chesapeak Bay form another example of a steep incised valley, filled with deposits that exhibit a more gentle slope. The longitudinal profiles for the Chesapeak Bay are interpreted from borings along the bay (Hack (1975)). Seismic analysis of the valley fill of the Gironde in South East France, allowed Lericolais (2001) to identify the seaward extension of the delta onto the continental shelf. The slope angles of lowstand and transgressive system tracts, again show a clear difference in slope is recognized.

Only Zaitlin et al (1994) recognize steeper transgressive ravinement slopes(high stand system tract), in their attempt to develop an idealized facies model for incised valley system.

Several explanations are proposed for the observed difference in longitudinal profile. The dominant assumption is that longitudinal profiles are dependent on changes in discharge of sediment, water or both and a previously determined profile set by basement or earlier erosional cycles. The role of base level fluctuation and the tendency of the system to aggrade or degrade to its equilibrium slope is often overlooked. Results presented in this report show that a fluctuation of sea level can produce a slope difference of 0.02 and the influence of eustacy on the topset slope should be incorporated in the interpretation of sedimentary systems.

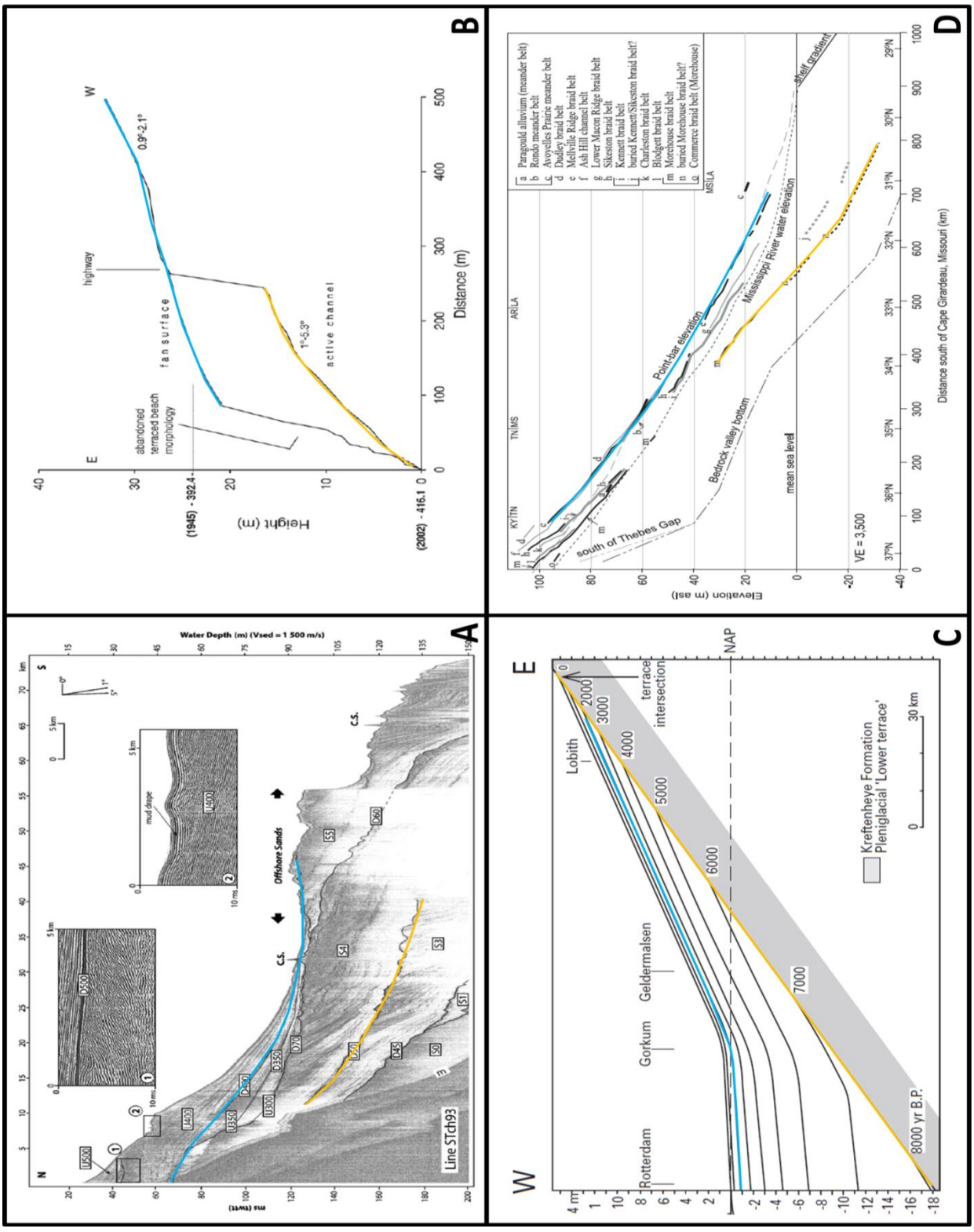

Figure 4. 2, Longitudinal fluvial profiles during transgressive system tracts and regressive system tracts. a. Rohne (Berné et al (2007)), b, desert streams near the Dead Sea (Bowman et al (2007)), Rhine-Meuse Delta (Berendsen (2005)) and d. Mississippi (Rittenour (2007)).

4.3.2 Buffers and buttresses

The base level buffers and buttresses model states that a sedimentary system can be defined by two bounding entities, each controlled by several forcing mechanisms. The buttress is the lowest point in the system, thus provides a limit to erosion of the system. This is often formed by sea level, but can also be formed by other base levels such as an unerodible basement for example. The fluvial profile that forms can be approached as a range of possible profiles, controlled by upstream variability such as sediment supply, tectonic uplift and water discharge. The buffer forms the range of all possible fluvial profiles (Holbrook (2006)). Shifting the buttress will have an effect on the fluvial profile, however within the ranges of the buffers. It is assumed that the covering parameters on the buffer work on longer timescales than the driving forces behind the buttress, e.g. eustacy acts on shorter time scales than tectonically driven changes in sediment budget. Therefore, buttress driven changes have a decreasing effect towards the proximal part of the buffer zone and constitute stronger effects downstream. Upstream the buffer will play a larger role. When incorporating this buttresses and buffers model in sequence stratigraphy, the preservation of fluvial strata and its internal architecture can be predicted by incorporating the upstream and downstream controls on the system (Holbrook (2006)).

The buffers and buttress model can be applied in to the experiments presented in this report. Two additions to the model can be proposed from the present report. The recognition of a system specific equilibrium slope, enables a concrete value to the fluvial profile and the buffers. The fluvial profile will fluctuate around the equilibrium slope. The equilibrium slope for a prograding system is lower, than its original static equilibrium slope. The second addition to the model is the role of base level variation in the governing processes of determining the buffers. During a sea level fall, when the system is erosive, the buffer actively shifts downward and becomes steeper. During sea level rise and the overall nature of the system is depostional, the buffers will move up. Incorporating this mechanism in the model, will add an integrated constraint on the buffer.

5. Conclusions

1. The changes applied with different frequencies indicate that the spatial scale of the system dictates its sensitivity to changes applied at different the time scales. Smaller systems are sensitive to short time scales and larger systems are affected by longer time scales. The high frequency applied changes dominantly affected the delta system and the low frequency changes affected only the larger shelf system. When changes are applied on time scale much larger than the systems characteristic equilibrium time, the system will develop a new equilibrium.

2. The dynamic topsets of both the shelf and the delta system are able to adapt their slope angles purely driven by sea level changes. An angle, smaller than the equilibrium gradient, develops during sea level rise, which is characteristic of a depositional system that allows aggradation of the topset. A large slope develops during sea level fall, an angle that exceeds the equilibrium angle characterizes an erosional system, with limited deposition on the topset and is dominantly progradational.

3. The buffering capacity of the subaerial topset slope is an important factor, determining the timing of the delta at the shelf edge. The topset slope is governed by several driving mechanisms. The three dominant forcing factors in the present report are; eustacy driven equilibrium slope grading, rate of progradation and sediment supply. Steep, straight slopes inhibit shoreline migration landward, furthermore, by the same sea level rise less accommodation space is created on those slopes.

6. Acknowledgements

First of all, I would like to thank Joris Eggenhuisen for giving me the opportunity, trust and freedom to set up this independent research in a new flume. I would like to thank Jochem Bijkerk for his endless enthusiasm and support and the many engaging discussions that we had in the past year. Matthieu Cartigny for helping me with the MATLAB analysis and demanding new and interesting movies every day. I thank all those who helped me during the process of writing this thesis. Wouter, Jan, Ronald, Eva, Tarek, Anna, Jort, Agnes, Joanna, Amalia and all the other students, with whom I've sheared so many coffee breaks and have made fun of my sandy playpen. And last but not least I would like to thank Marielle en Peter for believing in me, when I didn't myself.

References

Berendsen, H.J.A., (2005) The Rhine-Meuse delta at a glance, Utrecht University, ICG-report 2003/04, ISBN: 90-77079-13-0

Berendsen, H.J.A. and Stouthamer, E., (2001) Palaeogeographic development of the Rhine-Meuse delta, the Netherlands. ISBN 90 232 3695 5.

Berné, S., Jouet, G., Bassetti, M.A., Dennielou, B., Taviani, M. (2007) Late Glacial to Preboreal sea-level rise recorded by the Rhône deltaic system (NW Mediterranean), *Marine Geology,* 245, 65-88.

Blum, M.D. and Aslan, A. (2006). Signatures of climate vs. sea-level change within incised valley-fill successions: Quaternary examples of the Texas Gulf Coast. Sedimentary Geology, vol. 190, 177-211.

Bowman, D., Shachnovich-Firtel, Y., Shlomo, D., (2007) Stream channel convexity induced by continuous base level lowering, the Dead Sea, Israel, *Geomorphology*, 92, 60-75.

Burgess, P.M. and Hovius, N. (1998) Rates of delta progradation during highstands: consequences for timing of deposition in deep-marine systems, *Journal of the Geological Society*, Londen, UK., vol. **155**, pp. 217-222.

Castelltort, S. and Van den Driessche, J. (2003) How plausible are high-frequency sediment supply-driven cycles in the stratigraphic record?, *Sedimentary Geology,* Rennes, France, **157**, 3-13.

Catuneanu, O., Abreu, V., Bhattacharya, J.P., Blum, M.D., Dalrymple, R.W., Eriksson, P.G., Fielding, C.R., Fisher, W.L., Galloway, W.E., Gibling, M.R., Giles, K.A., Holbrook, J.M. Jordan, R., Kendall, C.G.St.C., Macurda, B., Martinsen, O.J., Miall, A.D., Neal, J.E., Nummedal, D., Pomar, L., Posamentier, H.W., Pratt, B.R., Sarg, J.F., Shanley, K.W., Steel, R.J., Strasser, A., Tucker, M.E., Winker, C. (2009) Reply to the comments of W. Helland-Hansen on "Towards the standardization of sequence stratigraphy" by Catuneanu et al. [Earth-Sciences Review 92 (2009) 1-33], *Earth-Science Reviews,* **94,** 98-100.

Catuneanu, O., Abreu, V., Bhattacharya, J.P., Blum, M.D., Dalrymple, R.W., Eriksson, P.G., Fielding, C.R., Fisher, W.L., Galloway, W.E., Gibling, M.R., Giles, K.A., Holbrook, J.M. Jordan, R., Kendall, C.G.St.C., Macurda, B., Martinsen, O.J., Miall, A.D., Neal, J.E., Nummedal, D., Pomar, L., Posamentier, H.W., Pratt, B.R., Sarg, J.F., Shanley, K.W., Steel, R.J., Strasser, A., Tucker, M.E., Winker, C. (2009) Towards the standardization of sequence stratigraphy, *Earth-Science Reviews*, **92**, 1-33.

Cohen, K.M., (2003) Diffenential subsidence within a coastal prism: Late-Glacial-Holocene tectonics in the Rhine-Meuse delta, The Netherlands, Utrecht, ISBN: 90-6809-354-1

Hack, J.T., (1957) Submerged river system of Chesapeake Bay, *Bulletin of the geological society of America*, Vol. 68, pp. 817-830

Helland-Hansen, W. and Hampson, G.J. (2009) Trajectory analysis: concepts and applications, *Basin Research*, 21, 454-483. doi: 10.1111/j. 1365-2117.2009.00425.x.

Helland-Hansen, W. and Martinsen, O.J. (1996) Shoreline Trajectories and Sequences: Description of Variable Depositional-Dip Scenarios, *Journal of Sedimentary Research*, Bergen, Norway, vol. **66**, No.4, p. 670-688.

Henriksen, S., Hampson, G.J., Helland-Hansen, W., Johannessen, E.P., Steel, R.J. (2009) Shelf edge and shoreline trajectories, a dynamic approach to stratigraphic analysis, *Basin research*, **21**, 445-453, doi: 10.1111/j.1365-2117.2009.00432.x.

Hijma, M.P., and Cohen, K.M., (2001) Holocene transgression of the Rhine river mouth area, The Netherlands/Southern North Sea: palaeogeography and sequence stratigraphy, *Sedimentology,* **58,** 1453-1485, doi: 10.1111/j.1365-3091.2010.01222.x.

Holbrook J. Scott, R.W., Oboh-Ikuenobe, F.E., (2006). Base-level buffers and buttresses: a model for upstream versus downstream control on fluvial geometry and architecture within sequences. *Journal of sedimentary research*, vol. 76, 162-174.

Hoyal, D.C.J.D. and Sheets, B.A. (2009) Morphodynamic evolution of experimental cohesive deltas, *Journal of Geophisical research,* vol. 114, F02009, doi: 10.1029/2007JF000882.

Imbrie, J. and Imbrie, J.Z., (1980). Modeling the Climatic Response to Orbital Variations. *Science, New Series,* American Association for the Advancement of Science, Vol. 207, No. 4434, pp. 943-953.
Imbrie, J. (1985). A theoretical framework for the Pleistocene ice ages, *Journal of the Geological Society,* v. 142, p 417-432. doi: 10.1144/gsjgs. 142.3.0417
Lai, S.Y.J. and Capart, H. (2007) Two-diffusion description of hyperpycnal deltas, *Journal of Geophisical research,* vol. **112**, F03005, doi: 10.1029/2006JF000617.
Lai, S.Y.J. and Capart, H. (2009) Resevoir infill by hyperpycnal deltas over bedrock, *Geophisical Research Letters,* vol. **36**, L08402, doi: 10.1029/2008GL037139.
Lericolais, G., Berné, S., Féniès, H. (2001) Seaward pinching out and internal stratigraphy of the Gironde incised valley on the shelf (Bay of Biscay), *Marine Geology,* 175, 183-197.
Loget, N., Davy, P., Driessche, J., Van Den. (2006) Mesoscale fluvial erosion parameters deduced from modeling the Mediterranean sea level drop during the Messinian (late Miocene), Journal of Geophysical research, Vol. 111, F03005, doi: 10.1029/2005JF000387.
Lorenzo-Trueba, J., Voller, V.R., Muto, T., Kim, W., Paola, C., Swenson, J.B. (2009) A similarity solution for a dual moving boundary problem associated with a coastal-plain depositional system, *J. Fluid Mech.* UK, vol. **628**, pp. 427-443.
Moshe, L.B., Haviv, I., Enzel, Y., Zilberman, E., Matmon, A., (2008) Incision of alluvial channels in response to a continuous base level fall: Field characterization, modeling, and validation along the Dead Sea, *Geomorphology,* 93, 524-536
Muto, T. and Steel, R.J. (2002) In Defence of Shelf-Edge Delta Development during Falling and Lowstand of Relative Sea Level, *The Journal of Geology,* Chicago, USA., vol. **110**, p. 421-436, 0022-1376/2002/11004-0004$15.00
Muto, T. (2001) Shorline Autoretreat Substantiated in Flume experiments, *Journal of Sedementery Research,* vol. **71**, No.2, p. 246-254, SEPM, 1073-130X/01/071-246/$03.00
Noorden van, L.P.E. ,. (2012) The influence of variations in excess density in hyperpycnal flows on the foreset angle of a delta,. Bsc Thesis Utrecht University
Paola, C., Hellert, P.L., Angevinet, C.L. (1992) The large-scale dynamics of grain-size variation in alluvial basins, 1: Theory, *Basin Research,* **4**, 73-90.
Paola, C., Straub, K., Mohrig, D., Reinhardt, L**.** (2009) The “unreasonable effectiveness” of stratigraphic and geomorphic experiments, *Earth-Science Reviews*, **97**, 1-43.
Parker, G., Muto, T., Akamatsu, Y., Dietrich, W.E., Lauer, J.W. (2008) Unravelling the conundrum of river response to rising sea-level from laboratory to field. Part II. The Fly-Strickland River system, Papua New Guinea, *Sedimentology,* **55**, 1657-1686, doi: 10.1111/j.1365-3091.2008.00962.x.
Pazzaglia, F.J., and Gardner, T.W., (1993) Fluvial terraces of the lower Susquehanna River, *Geomorphology,* Elsevier Science Publishers BV, 8, 83-113
Posamentier, H.W., Allen, G.P., James, G.P., Tesson, M. (1992) Forced Regressions in a Sequence Stratigraphic Framework: Concepts, Examples, and Exploration Significance, *The American Association of Petroleum Geologists Bulletin,* V.**76**, No.11, P.1687-1709, 18.Figs, 1.Table
Postma, G., Kleinhans, M.G., Meijer, P.Th. and Eggenhuisen, J.T. (2008). Sediment transport in analogue flume models compared with real-world sedimentary systems: a new look at scaling evolution of sedimentary systems in a flume. *Sedimentology*, vol. 55, 1541-1557.
Rittenour, T.M., Blum, M.D., Goble, R.J., (2007) Fluvial evolution of the lower Mississippi River valley during the last 100 k.y. glacial cycle: Response to glaciation and sea-level change, *Geological Society of America Bulletin,* v.119, no. 5/6, p. 586-608, doi: 10.1130/B25934.1
Reading, H.G,. (1996) Sedimentary Environments: Processes, Facies and Stratigraphy, third edition. Blackwell publishing ISBN: 978-0-6320-3627-1
Schlager, W. (2010) Ordered hierarchy versus scale invariance in sequence stratigraphy, *It J Earth Sci (Geol Rundsch)*, **99**, (supl. 1):S139-S151, doi: 10.1007/s00531-009-0491-8

Schlager, W. (1993) Accommodation and supply-a dual control on stratigraphic sequences, *Sedimentary Geology*, Amsterdam, The Neth erlands, **86**, 111-136.
Swenson, J.B. and Muto, T. (2007) Response of coastal plain rivers to falling relative sea-level: allogenic controls on the aggrodational phase, *Sedimentology,* **54**, 207-221, doi: 10.1111/j.1365-3091.2006.00830.x.
Törnqvist, T.E., (1998) Longitudinal profile evololution of the Rhine-Meuse system during the last deglaciation: interplay of climate change and glacioeustasy?, *Terra Nova,* Blackwell Science Ltd, Vol **10**, No. 1, 11-15.
Zaitlin, B.A., Dalrymple, R.W., Boyd, R., (1994) The stratigraphic organization of incised-valley systems associated with relative sea-level change, *SEPM Special Publication,* No. 51, ISBN: 1-56576-015-8

Appendix 1. Equilibrium runs.

To test what settings fit the experiments best, a series of equilibrium runs was performed. With these equilibrium runs it was determined what amounts of sediment, the composition of the sediment and the volume of the water that is going to be used. Furthermore, het nature of the applicable transport equation was determined. The equilibrium experiments are preformed in a 0,05 m wide, approximately 2m long and 0,80 m high flume. *The sand is delivered to a gravel basket at the beginning of the tank by a screw feeder and mixed in a funnel with the water that enters the flume*. The end of the depositional system is marked by a wooden barrier where the water and sediment can flow freely, preventing the system from prograding and thereby keeping the length scale constant. The water surface of the receiving tank was kept constant and below the wooden barrier, which formed base level, for all the equilibrium experiments.

The first equilibrium started with 250 dm^3/h water and 1 dm^3/h of sediment, however these settings resulted in cyclic steps and chute and pools. Runs where 150 dm^3/h water was used resulted in focus of flow and small scale meandering behavior, since the interest here is in the overall behavior of the system and not the small scale autogenic variability, this water discharge was also abandoned.

For a sediment composition of pure sand, a water discharge of 200 dm^3/h appears to provide an equally distributed flow over the sediment surface for all amounts of sediment discharge, ranging from 1 – 3 dm^3/h (table 1).

	EQ9	EQ12	EQ10	EQ13	EQ11
Qw (m2/sec)	1,1E-3	1,1E-3	1,1E-3	1,1E-3	1,1E-3
Qs (m2/sec)	5,6E-6	8,3E-6	1,1E-5	1,4E-5	1,7E-5
Seq	0,02875	0,0360	0,0414	0,0455	0,0518
water temp(°C)	12,7	12,4	12,7	12,4	12,8

Table 1, Overview of equilibrium runs and associated sediment supply, water discharge and equilibrium slope.

Using the sediment discharge and the equilibrium slope, the diffusivity can be determined (figure 1). Here the equation $Qs = v * S_{eq}^{m}$ can be used. Where Qs is the sediment discharge in m^2/sec, v is the diffusivity in m^2/sec and S_{eq} represents the equilibrium slope that is developed. As can be seen in figure 1 the diffusivity of the pure sand equilibrium runs is $4.9 * 10^{-3}$ m^2/sec.

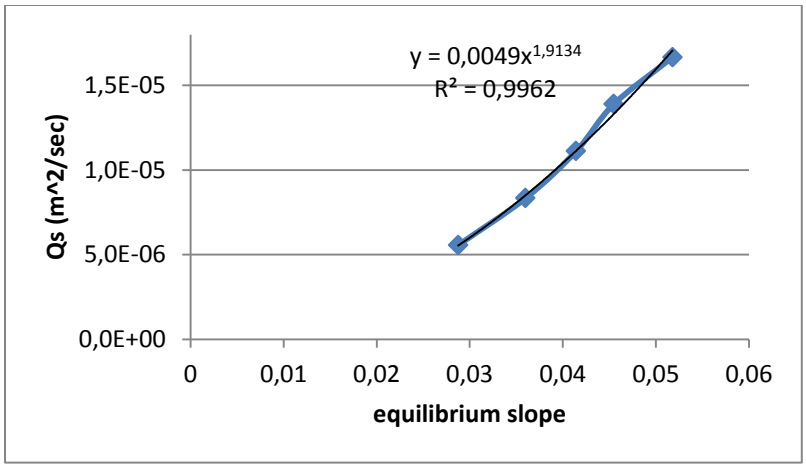

Figure 1, diffusivity determined with use of sediment discharge and the developed equilibrium slope.

With this information the equilibrium times of the same runs can be calculated (figure 2), using : $T_{eq} = H*L / Q_s$, where T_{eq} represents the equilibrium time in sec, H determines the height of the sediment surface and L the length of the system.

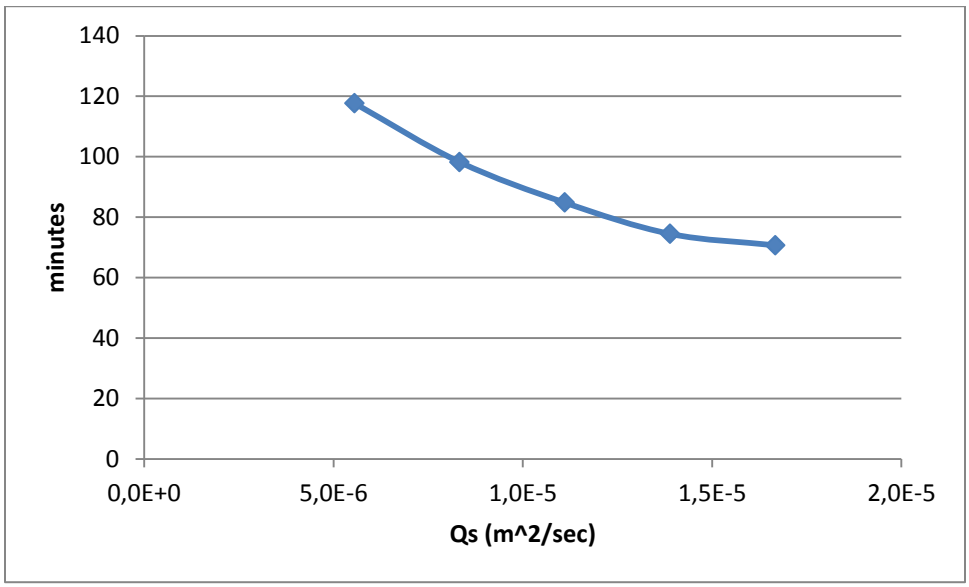

Figure 2, equilibrium times determined from the volume of the sediment wedge and the sediment discharge.

Figure 2 shows that the equilibrium times decrease with increasing sediment discharge. However since the equilibrium time is primarily dependent on the diffusivity and diffusivity is dependent on the water discharge; one would expect equilibrium times to remain constant for all five experiments. Furthermore, figure 3 shows the normalized sediment heights for these equilibrium runs and these graphs appear to be showing a similar equilibrium time for all experiments.

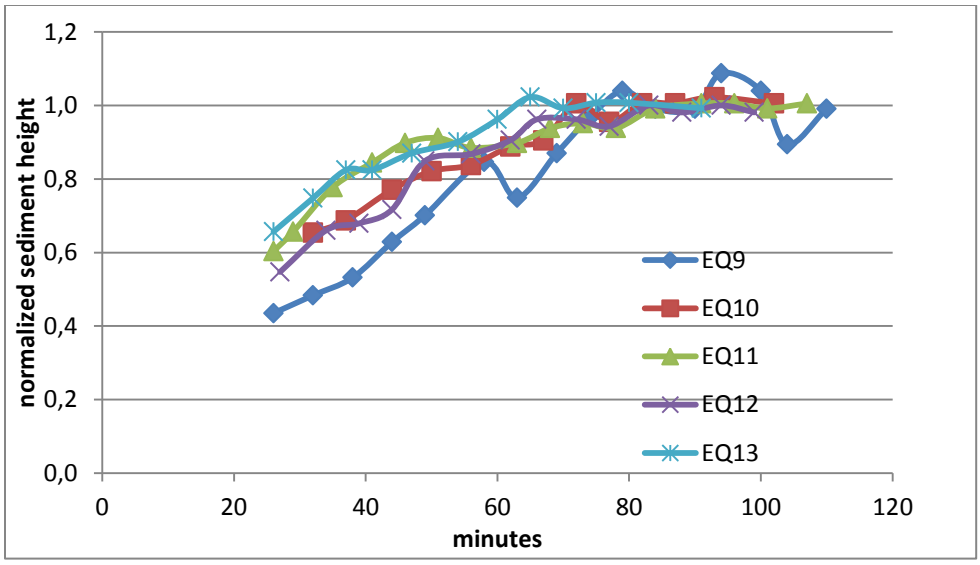

Figure 3, normalized sediment height for the equilibrium runs.

From figure 2 it becomes apparent that the linear diffusion equation is not valid for this type of experiment and that further research needs to be conducted. However, for simplicity of the experiments linear diffusivity will be assumed. Assuming an equilibrium slope of 0.0414 for a sediment discharge of 2 l/hr and a water discharge of 200 l/hr, with a fixed length for the system, this results in an equilibrium time of 62.7 minutes. According to equation 9 by Postma et al. (2008); $T_{eq} = \frac{H*L}{Q_s}$.

Appendix 2, summary table experiments

		sea level curve				sediment supply			experimental set up	
			subidence							frequency applied changes
		period	amplitude	component	symetry	period	amplitude	symetry	duration	
sea level experiments	SL_HF_A1	1 hr	1.25 cm	--	assymetircal fast increase	--	--	--	4 hr	5 min
	TR	1 hr	1.25 cm	--	assymetircal fast increase	--	--	--	2 hr	1 min
	SL_HF_A3	1 hr	1.25 cm	1 cm/hr	assymetircal fast increase	--	--	--	4 hr	5 min
	SL_LF_A1	4 hr	1.25 cm	--	assymetircal fast increase	--	--	--	4 hr	5 min
	SL_LF_A3	4 hr	1.25 cm	1cm/hr	assymetircal fast increase	--	--	--	4 hr	5 min
sediment supply experiments	QS_HF_A1	--	--	--	--	1 hr	1 l/hr	assymetrical fast increase	2 hr	5 min
	Qs_HF_A7	--	--	--	--	1 hr	1 l/hr	assymetrical fast decrease	2 hr	5 min
	QS_LF_A1	--	--	--	--	4 hr	1 l/hr	symetrical	4 hr	5 min
combined experiments	CO1_HF_A3	1 hr	1.25 cm	1 cm/hr	assymetircal fast increase	1 hr	1 l/hr	assymetrical fast increase	4 hr	5 min
	CO2_HF_A3	1 hr	1.25 cm	1 cm/hr	assymetircal fast increase	1 hr	1 l/hr	assymetrical fast decrease	4 hr	5 min
	CO3_HF_A3	1 hr	1.25 cm	1 cm/hr	assymetircal fast increase	4 hr	1 l/hr	symetrical	4 hr	5 min